Electronic Supplementary Material (ESI) for Dalton Transactions.

Supporting Information for Spin-State Control of Cobalt(II) and Iron(II) Complexes with Click-Derived Tripodal Ligands Through Non-Covalent and Fluorine-Specific Interactions

Content

Experimental Section	S1
Magnetometric Measurements	S8
HF-EPR Measurements	S11
Mössbauer Spectroscopy	S13
UV/Vis Spectroscopy	S13
IR Spectroscopy	S14
X-Ray Crystallography	S17
Computational Details	S19
NMR Spectra	S21
References	S27

Experimental Section

General Remarks and Instrumentation. If noted, reactions were carried out using standard Schlenk-line techniques under an inert atmosphere of argon (Linde, HiQ Argon 5.0, purity ≥99.999%). Compounds: The ligands TF_3TA and TF_5TA were synthesized by a Cu(I) catalyzed "click" reaction,[1] ligand $MBDF_5TA$ and all complexes were synthesized following published procedures.[2, 3] Commercially available chemicals were used without further purification. ^1H NMR and proton decoupled ^{13}C NMR were recorded on JEOL ECS 400 spectrometer and JEOL ECZ 400R spectrometer at 20 °C. Chemical shifts are reported in ppm (relative to the TMS signal) with reference to the residual solvent peaks.[4] Multiplets are reported as follows: singlet (s), doublet (d), triplet (t), quartet (q), quintet (quint), septet (sept), and combinations thereof. Mass spectrometry was performed on an Agilent 6210 ESI-TOF. Elemental analysis was performed on a Perkin Elmer Analyser 240.

X-ray diffraction

X-ray data were collected on a Bruker Smart AXS or Bruker D8 Venture system at 100(2) K, respectively, using graphite-monochromated Moα radiation (λ_α = 0.71073 Å). Using the Smart software or using the APEX2 software, respectively, evaluated the strategy for the data collection. The data were collected by the standard omega scan or omega + phi scan techniques, and were scaled and reduced using Saint + and SADABS software. Direct methods or intrinsic phasing using SHELXT-2014/7 solved the structures. Structures were refined by full matrix least-squares using SHELXL-2014/7, refining on F2. Non-hydrogen atoms were refined 40 anisotropically.[5-11]

SQUID Magnetometry

All susceptibility measurements were carried out on a Quantum Design MPMS3 SQUID magnetometer. The measurements at a constant magnetic field of 1000 Oe in a temperature range from 1.8 K to 50 K and at 10 000 Oe in a temperature range from 40 K to 300 K. The measured data in the intersection of the temperature ranges served to compensate for possible ferromagnetic impurities. Samples were either pressed into a pellet with a diameter of 5 mm and fixed in a plastic tube or pounded with little pressure and mixed with eicosane. The mixture was melted in a capsule with a hot air gun maximized to a temperature of 50 °C (323.15 K) and the capsule was then fixed in a plastic tube. The temperature dependent measurements were limited to a temperature of 300 K due to the melting of the used eicosane matrix (melting point of eicosane: 311 K). For all samples, an immobilization in eicosane was the preferable method, since in the case of **FeTF5E**, it was found, that pressing a pellet is leading to a loss of the SCO properties. Consequently, Cobalt samples were only prepared in eicosane matrix.

Data were corrected for the diamagnetic contribution to the susceptibility by means of Pascal's constants.[12]

High-Frequency EPR spectroscopy

HFEPR measurements were carried out on a home-built spectrometer, equipped with a 15 T Oxford magnet.[13] Same samples as in the case of the SQUID magnetomery measurements were used.

Mössbauer spectrosopy

Mössbauer measurements were performed using an MS96 spectrometer from RCPTM coupled to a Janis SVT-400 bath cryostat. A M.Co7.124 57Co isotope (in Rh-Matrix) from Ritverc with a nominal activity of 1850 MBq was used as the source. Calibration of the velocity axes was performed against α-iron at room temperature. Spectra were fitted using the *MossWinn 4.01* software. In order to reduce the mechanical stress on the samples, samples were prepared as loose powders, wrapped in weighing paper that was folded to a square with an area of 10 mm x 10 mm. After securing with parafilm, the sample was fixed in a home made aluminum sample holder, attached to the sample rod.

Synthesis

Caution! *Organic azides are potentially explosive. Although we never experienced any problems during synthesis or analysis, all compounds should be synthesized only in small quantities and handled with great care.*

2,4,6-Trifluorobenzylazide

2,4,6-trifluorobenzylbromide (10.1 g, 45.0 mmol), NaN_3 (5.9 g, 90.0 mmol) and KI (149.4 mg, 0.9 mmol) were dissolved in MeOH (30 mL) and H_2O (30 mL) and heated to reflux for 1 day. The mixture was cooled to room temperature and 30 mL H_2O were added and extracted with Et_2O (3 · 100 mL). The organic phase was dried over Na_2SO_4 and the solvent was removed under reduced pressure yielding a yellow oil (7.2 g, 38.8 mmol, 86%).

^{1}H NMR ($CDCl_3$, 401 MHz, 21 °C): δ = 6.76 – 6.70 (m, 2H), 4.38 (s, 2H) ppm.

^{13}C NMR ($CDCl_3$, 401 MHz, 20 °C): δ = 144.6 (c, triazol), 144.2 (C, triazol), 134.8 (C, benzyl), 129.2 (CH, benzyl), 128.8 (CH, benzyl), 128.1 (CH, benzyl), 124.2 (CH, triazol), 123.9 (CH, triazol), 54.3 (CH_2), 47.2 (CH_2), 47.0 (CH_2), 40.9 (CH_2) ppm

^{19}F NMR ($CDCl_3$, 401 MHz, 21 °C): δ = 6.76 – 6.70 (m, 2H), 4.38 (s, 2H) ppm.

Pentafluorobenzylazide

Pentafluorobenzylbromide (11.7 g, 45.0 mmol), NaN_3 (5.9 g, 90.0 mmol) and KI (149.4 mg, 0.9 mmol) were dissolved in MeOH (30 mL) and H_2O (30 mL) and heated to reflux for 1 day. The mixture was cooled to room temperature and 30 mL H_2O were added and extracted with Et_2O (3 · 100 mL). The organic phase was dried over Na_2SO_4 and the solvent was removed under reduced pressure yielding a yellow oil (7.6 g, 34.0 mmol, 76%).

The ^{1}H-NMR spectrum corresponds to literature.[14]

^{1}H NMR ($CDCl_3$, 401 MHz, 20 °C): δ = 4.46 (s, 2H) ppm.

(1-benzyl-1H-1,2,3-triazol-4-yl)methanamine

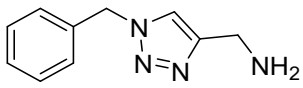

To a solution of propargyl amine (560 mg, 10 mmol) and benzylazide (1.6 g, 12 mmol) in dry DCM (40 mL) were added 1-butyl-3-isopropyl-1H-benzo[d]imidazole-3-iumbromide (74 mg, 2.5mol-%), CuI (48 mg, 2.5 mol-%) and KO^{t}Bu (48 mg, 3.75 mol-%). The mixture was sonicated for 1 h and afterwards stirred at room temperature for 3 d. The addition of a $H_2EDTANa_2$ solution (ca. 0.5 g) in aqueous ammonia (ca 5%, 15 mL) stopped the reaction. The aqueous phase was extracted with DCM (3 · 30 mL) and the combined organic phases were washed with distilled water and dried over Na_sSO_4. After removal of the solvent under reduced pressure, the crude product was purified by column chromatography (basic aluminum oxide). The eluent slowly changed from DCM (azide) to ethylacetate and finally to methanol. The product (1-benzyl-1H-1,2,3-triazol-4-yl)methanamine was obtained as yellow solid (1.15 g, 0.9 mmol, 61% yield).

The ^{1}H-NMR spectrum corresponds to literature.[2]

^{1}H NMR (acetone-d^6, 401 MHz, 21 °C): δ = 7.75 (s, 1H), 7.45 – 7.41 (m, 2H), 7.17 – 7.12 (m, 1H), 5.59 (s, 2H), 4.43 (s, 1H) ppm.

1-(1-benzyl-1H-1,2,3-triazol-4-yl)-N,N-bis((1-((perfluorophenyl)methyl)-1H-1,2,3-triazol-4-yl)methyl)methanamine (MBDF$_5$TA)

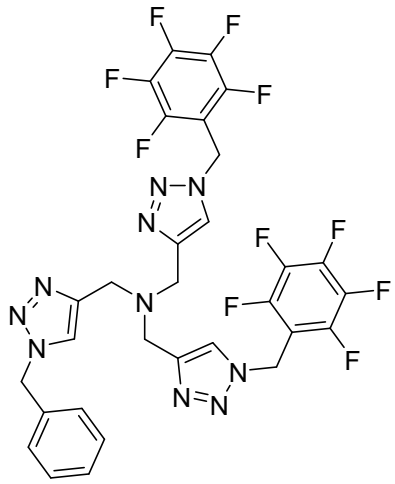

(1-benzyl-1H-1,2,3-triazol-4-yl)methanamine (545.9 mg, 2.9 mmol) and propargylbromide (9.0 mmol, 80 wt-% in toluene, 1.0 mL) were dissolved in dry THF (20 mL) and K_2CO_3 (3.5 g, 25 mmol) was added. The mixture was stirred for 1 d at room temperature and after addition of another portion of propargylbromide (0.3 mL) the mixture was stirred for another day. After inert filtration the solvent was removed under reduced pressure to obtain N-((1-benzyl-1H-1,2,3-triazol-4-yl)methyl)-N-(prop-2-yn-1-yl)prop-2-yn-1- as brown oil. The subsequent Click reaction was done without further purification.

To a solution of N-((1-benzyl-1H-1,2,3-triazol-4-yl)methyl)-N-(prop-2-yn-1-yl)prop-2-yn-1-amine in dry DCM (15 mL) were added 2,3,4,5,6-pentafluorobenzylazide (1.4 g, 6.1 mmol), 1-butyl-3-isopropyl-1H-benzo[d]imidazole-3-iumbromide (37.0 mg, 2.5mol-%), CuI (24.0 mg, 2.5 mol-%) and KO^{t}Bu (24.0 mg, 3.75 mol-%). The mixture was sonicated for 1 h and afterwards stirred at room temperature for 2 d. The crude product was purified by column chromatography (basic Al_2O_3, DCM (azide) to DCM/MeOH 10:1). Afterwards the pure product was obtained from precipitation of the crude product in DCM into Et_2O/*n*-pentane as a colorless solid (530.0 mg, 0.7 mmol, 26% with respect to the (1-benzyl-1H-1,2,3-triazol-4-yl)methanamine.

^{1}H NMR ($CDCl_3$, 401 MHz, 20 °C): δ = 7.83 (s, 2H), 7.65 (s, 1H), 7.40 – 7.31 (m, 3H), 7.27 (s, 1H), 7.25 (d, J = 1.8 Hz, 1H) 5.60 (s, 4H), 5.51 (d, J = 2.9 Hz, 2H), 3.71 (s, 6H) ppm.

^{13}C NMR ($CDCl_3$, 401 MHz, 20 °C): δ = 144.6 (c, triazol), 144.2 (C, triazol), 134.8 (C, benzyl), 129.2 (CH, benzyl), 128.8 (CH, benzyl), 128.1 (CH, benzyl), 124.2 (CH, triazol), 123.9 (CH, triazol), 54.3 (CH_2), 47.2 (CH_2), 47.0 (CH_2), 40.9 (CH_2) ppm

HRMS (ESI): calcd. For $[C_{30}H_{19}F_{10}N_{10}Na]^+$: *m/z* 733.1605; found 733.1552.

Anal. Calcd for $C_{30}H_{20}F_7N_{10} \cdot 0.6\ CH_2Cl_2$: C, 48.26; H, 2.81; N, 18.39. Found: C, 47.38; H, 2.85; N, 19.34.

Tris((1-(2,4,6-trifluorobenzyl)-1H-1,2,3-triazol-4-yl)methyl)amine (TF_3TA)

2,4,6-trifluorobenzylazide (2.1 g, 11.3 mmol), tripropargylamine (491.9 mg, 3.8 mmol) and $CuSO_4 \cdot 5H_2O$ (187.3 mg, 0.8 mmol) were placed in a round-bottom flask and 30 mL MeOH/H_2O (7:1) were added. The mixture was sonicated for 5 min and afterwards sodium ascorbate (297.8 mg, 1.5 mmol) was added. The mixture was again sonicated for 3 h and stirred overnight. To the reaction mixture 40 mL DCM was added and extracted with EDTA solution (3 · 40 mL). The organic phase was dried over Na_2SO_4 and the solvent was evaporated. The pure product was obtained from precipitation of the crude product in DCM into Et_2O/*n*-pentane as a colorless solid (803 mg, 1.2 mmol, 31%).

^{1}H NMR ($CDCl_3$, 400 MHz, 22 °C): δ = 7.75 (s, 1H), 6-76 – 6.69 (m, 2H), 5.53 (s, 2H), 3.68 (s, 2H) ppm

^{13}C NMR ($CDCl_3$, 101 MHz, 22 °C): δ = 174.06, 174.03, 164.56, 163.17, 163.07, 162.93, 160.66, 160.57, 160.52, 160.42, 143.29, 123.90, 107.69, 107.65, 107.50, 107.45, 107.31, 107.26, 101.25, 101.22, 100.99, 100.95, 100.72, 100.69, 100.13, 100.12, 47.01, 41.70 ppm

HRMS (ESI): calcd. For $[C_{30}H_{22}F_9N_{10}]^+$: *m/z* 693.1880; found 693.1913.

Anal. Calcd for $C_{30}H_{21}F_9N_{10}$: C, 52.03; H, 3.06; N, 20.23. Found: C, 52.37; H, 3.331; N, 20.51.

Tris[(1-pentafluorbenzyl-1*H*-1,2-3-triazol-4yl)methyl]-amine (TF_5TA)

Pentafluorobenzylazide (1 g, 4.5 mmol), tripropargylamine (147 mg, 1.12 mmol), $CuSO_4 \cdot 5H_2O$ (50 mg, 0.168 mmol) and TBTA (9 mg, 0.0168 mmol) were placed in a round-bottom flask and 90 mL DCM/$H_2$0/*tert*-butanol (1:1:1) were added. Then sodium ascorbate (106 mg, 0.67 mmol) was added and the reaction was stirred at 70 °C for 4 days. To the reaction mixture 20 mL water was added and extracted with DCM (3 · 40 mL). Then the combined organic phases were washed with washed with aqueous ammonia (ca. 50%, 5 · 30 mL) and finally with water (2 ·50 mL). The organic phases were dried over Na_2SO_4 and the solvent was evaporated. The pure product was obtained from precipitation of the crude product in DCM into Et_2O/*n*-pentane as a colorless solid (850 mg, 1.06 mmol, 95%).

^{1}H NMR ($CDCl_3$, 600 MHz, 25 °C): δ = 7.81 (s, 3H), 5.61 (s, 6H), 3.72 (s, 6H) ppm

^{13}C NMR ($CDCl_3$, 151 MHz, 25 °C): δ = 146.40, 144.74, 144.47, 141.40, 138.67, 137.00, 124.07, 108.37, 47.03, 40.93 ppm

^{19}F NMR ($CDCl_3$, 565 MHz, 25 °C): δ = -141.64, -150.93, -160.03 ppm

HRMS (ESI): calcd. For $[C_{30}H_{15}F_{15}N_{10}Na]^+$: *m/z* 823.1134; found 823.1159.

Anal. Calcd for $C_{30}H_{15}F_{15}N_{10} \cdot 0.25\ C_4H_{10}O$: C, 45.46; H, 2.15; N, 17.10. Found: C, 45.61; H, 2.52; N, 17.50.

$[Co(TF_5TA)_2](BF_4)_2$ (CoTF5): $Co(BF_4)_2 \cdot 6\ H_2O$ (29 mg; 0.085 mmol) and TF_5TA (136.1 mg; 0.17 mmol) were placed in a Schlenk tube and propylene glycol (3.2 mL) was added. Prior to the reaction argon was bubbled through the reaction mixture for 5 min. Then the Schlenk tube placed in an oil bath at 130 °C and stirred for 1 h. The reaction mixture was allowed to cool down in the oil bath overnight. A precipitate was filtered off and the pink filtrate was collected. Then Et_2O (6 mL) was added and the mixture was shaken properly. After several days pink single crystalline product could be collected. (19 mg, 0.01 mmol, 11%). The sample which was submitted to elemental analysis was washed with Et_2O. Anal. Calcd for $C_{60}H_{30}B_2CoF_{38}N_{20}$: C, 39.30; H, 1.65; N, 15.28. Found: C, 39.34; H, 1.88; N, 15.43.

$[Co(TF_5TA)_2](BF_4)_2 \cdot 2MeOH$ (CoTF5M): $Co(BF_4)_2 \cdot 6\ H_2O$ (32 mg; 0.095 mmol) and TF_5TA (152 mg; 0.19 mmol) were placed in a Schlenk tube and MeOH (6 mL) was added. Prior to the reaction argon was bubbled through the reaction mixture for 5 min. Then the Schlenk tube placed in an oil bath at 70 °C and stirred for 1 h. The reaction mixture was allowed to cool down in the oil bath overnight. The precipitate contained the pink single crystalline product $[Co(TF_5TA)_2](BF_4)_2 \cdot 2$ MeOH which was collected by filtration (134.0 mg; 0.07 mmol; 74%). Anal. Calcd for: $C_{60}H_{30}B_2CoF_{38}N_{20} \cdot 2\ CH_4O$: C, 39.24; H, 2.02; N, 14.76. Found: C, 39.55; H, 2.041; N, 14.84.

$[Co(TF_5TA)_2](BF_4)_2 \cdot 2EtOH$ (CoTF5E): $Co(BF_4)_2 \cdot 6\ H_2O$ (21.2 mg; 0.063 mmol) and TF_5TA (100 mg; 0.125 mmol) were placed in a Schlenk tube and EtOH (4 mL) and MeCN (0.15 mL) was added. Prior to the reaction argon was bubbled through the reaction mixture for 5 min. Then the Schlenk tube placed in an oil bath at 80 °C and stirred for 1 h. The reaction mixture was allowed to cool down in the oil bath overnight. A precipitate was obtained by slow diffusion of Et_2O into the reaction mixture and contained the pink single crystalline product $[Co(TF_5TA)_2](BF_4)_2 \cdot 2$ EtOH which was collected by filtration (68.0 mg; 0.03 mmol; 56%). Anal. Calcd for: $C_{60}H_{30}B_2CoF_{38}N_{20} \cdot 2C_2H_6O$: C, 39.92; H, 2.20; N, 14.55. Found: C, 39.98; H, 2.20; N, 14.75.

$[Co(TF_5TA)_2](BF_4)_2 \cdot 1.5$toluene$\cdot 0.5Et_2O$ (CoTF5T): A solution of toluene (5.5 mL) and MeCN (0.3 mL) was degassed for 5 min in a Schlenk tube. $Co(BF_4)_2 \cdot 6H_2O$ (32.4 mg; 0.095

mmol) and TF_5TA (152.3 mg; 0.19 mmol) were added. Then the Schlenk tube placed in an oil bath at 100 °C and stirred for 1 h. The reaction mixture was allowed to cool down in the oil bath overnight. The pink single crystalline product $[Co(TF_5TA)_2](BF_4)_2 \cdot 1.5\ C_7H_8 \cdot 0.5\ Et_2O$ was obtained by slow diffusion of Et_2O into the reaction mixture (83.0 mg; 0.04 mmol; 45%). Anal. Calcd for : $C_{60}H_{30}B_2CoF_{38}N_{20} \cdot 0.5C_4H_{10}O \cdot 1.55C_7H_8$: C, 43.90; H, 2.59; N, 13.63. Found: C, 43.54; H, 2.21; N, 13.25.

$[Co(TF_5TA)_2](BF_4)_2 \cdot 1.5$fluorobenzene$\cdot 0.5\ Et_2O$ (CoTF5F): A solution of fluorobenzene (4 mL) and MeOH (1.5 mL) was degassed for 5 min in a Schlenk tube. $Co(BF_4)_2 \cdot 6H_2O$ (32.8 mg; 0.095 mmol) and TF_5TA (152 mg; 0.18 mmol) were added. Then the Schlenk tube placed in an oil bath at 85 °C and stirred for 1 h. The reaction mixture was allowed to cool down in the oil bath overnight. The pink single crystalline product $[Co(TF_5TA)_2](BF_4)_2 \cdot 1.5\ C_6H_5F \cdot 0.5\ Et_2O$ was obtained by slow diffusion of Et_2O into the reaction mixture (87.6 mg; 0.05 mmol; 48%). Anal. Calcd for: $C_{60}H_{30}B_2CoF_{38}N_{20} \cdot 1.9CH_4O \cdot 0.8C_6H_5F$: C, 40.64; H, 2.13; N, 14.21. Found: C, 40.28; H, 1.76; N, 13.85.

$[Co(TF_3TA)_2](BF_4)_2 \cdot 2$MeOH (CoTF3M): $Co(BF_4)_2 \cdot 6\ H_2O$ (29 mg; 0.085 mmol) and TF_3TA (117 mg; 0.17 mmol) were placed in a Schlenk tube and methanol (6 mL) was added. Prior to the reaction argon was bubbled through the reaction mixture for 5 min. Then the Schlenk tube was placed in an oil bath at 70 °C and stirred for 1 h. After removing the stirring bar from the solution the reaction was allowed to cool down in the oil bath overnight. The precipitate obtained by slow diffusion of Et_2O in the reaction mixture contained the pink single crystalline product $[Co(TF_3TA)_2](BF_4)_2 \cdot 2$ MeOH which was collected by filtration (108.1 mg; 0.06 mmol; 76%). Anal. Calcd for $C_{60}H_{42}B_2CoF_{26}N_{20} \cdot 2CH_4O$: C, 44.28; H, 3.00; N, 16.66. Found: C, 44.49; H, 3.05; N, 16.84.

$[Co(MBDF_5TA)_2](BF_4)_2$ (CoBF5): A solution of MeOH (2 mL) was degassed for 5 min in a Schlenk tube. $Co(BF_4)_2 \cdot 6H_2O$ (29 mg; 0.085 mmol) and $MBDF_5TA$ (120.8 mg; 0.17 mmol) were added. Then the Schlenk tube placed in an oil bath at 70 °C and stirred for 1 h. The reaction mixture was allowed to cool down in the oil bath overnight. The pink single crystalline product $[Co(MBDF_5TA)_2](BF_4)_2 \cdot$ was obtained by slow diffusion of Et_2O into the reaction mixture (44.3 mg; 0.03 mmol; 32%). Anal. Calcd for: $C_{60}H_{49}B_2CoF_{28}N_{20}$: C, 43.58; H, 2.44; N, 16.94. Found: C, 43.58; H, 2.24; N, 16.65.

[Fe(TF$_5$TA)$_2$](BF$_4$)$_2$·2EtOH (FeTF5E): Fe(BF$_4$)$_2$·6H$_2$O (31.8 mg; 0.09 mmol) and TF$_5$TA (152.1 mg; 0.19 mmol) were dissolved in EtOH (5 mL) and stirred at 80 °C 1 h. The reaction mixture was allowed to cool down in the oil bath overnight. Diffusion of Et$_2$O into the reaction mixture yielded in the yellow single crystalline product [Fe(TF$_5$TA)$_2$](BF$_4$)$_2$ · 2 EtOH which was collected by filtration (102.1 mg; 0.05 mmol; 59%). Anal. Calcd for: C$_{60}$H$_{30}$B$_2$FeF$_{38}$N$_{20}$· 2C$_2$H$_6$O: C, 39.98; H, 2.20; N, 14.57. Found: C, 40.00; H, 2.24; N, 14.59.

Magnetometric Measurements

Figure S1: Preparation of the samples. Top: compound in eicosane matrix in plastic capsule. Bottom: compound pounded and pressed into a pellet. For **FeTF5E**, temperature dependent magnetic measurements were carried out on both sample preparation methods. Here, it was found, that pressing a pellet is leading to a partial loss of the SCO property (figure S4). Consequently, following measurement on the Co compounds were only carried out on samples immobilized in eicosane.

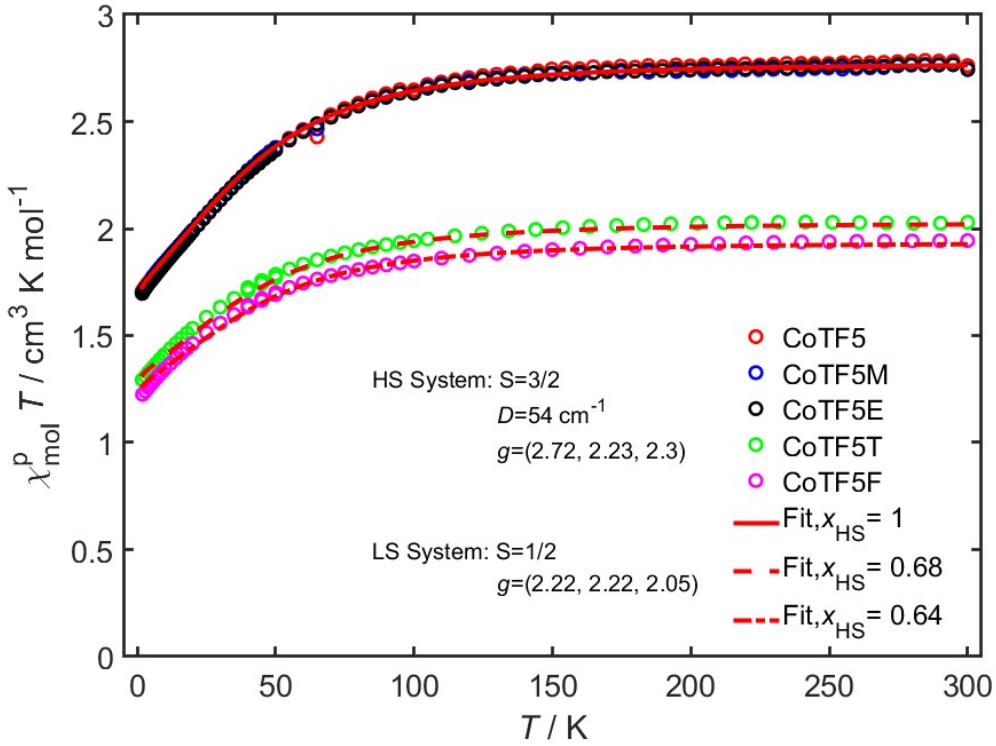

Figure S2: Temperature susceptibility product as a function of temperature of compounds **CoTF5-CoTF5F** of eicosane immobilized samples. The corresponding fits were done with the spin-Hamiltonian parameters shown in the figure. From the simulation of compound **CoTF5T** and **CoTF5F**, it gets clear, that high spin and low spin species are coexisting.

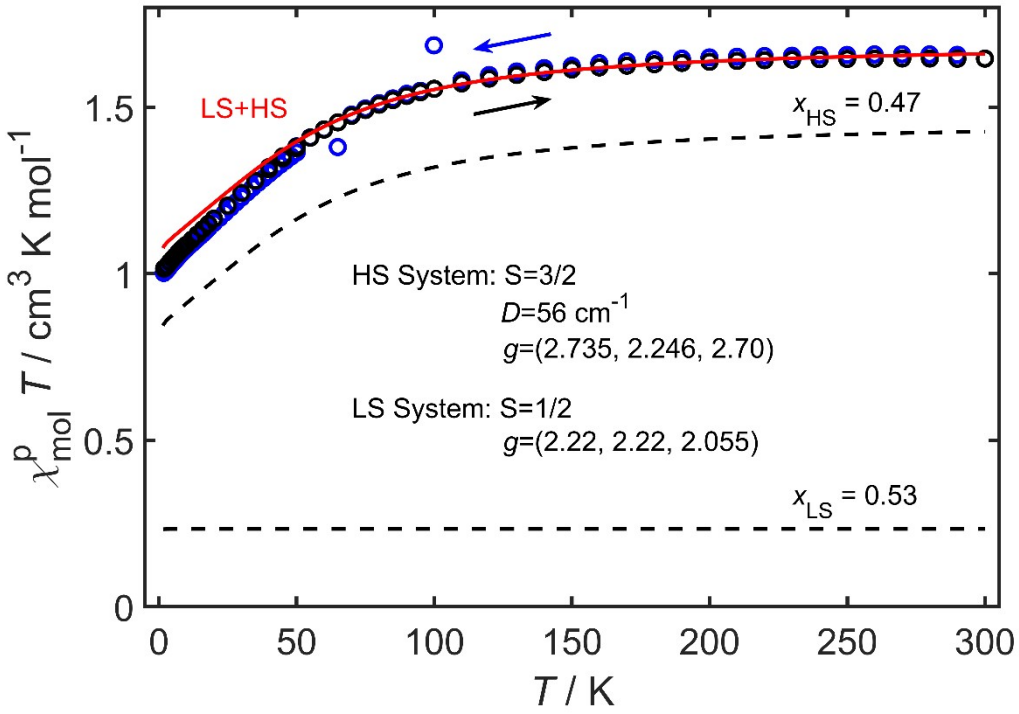

Figure S3: Susceptibility temperature product as a function of the temperature of **CoTF3M**, immobilized in eicosane**.** Sweeping direction of temperature sweeps is indicated by arrows. The parameters of the corresponding spin-Hamiltonian fits are shown in the figure. The fits are shown as red straight and dashed lines.

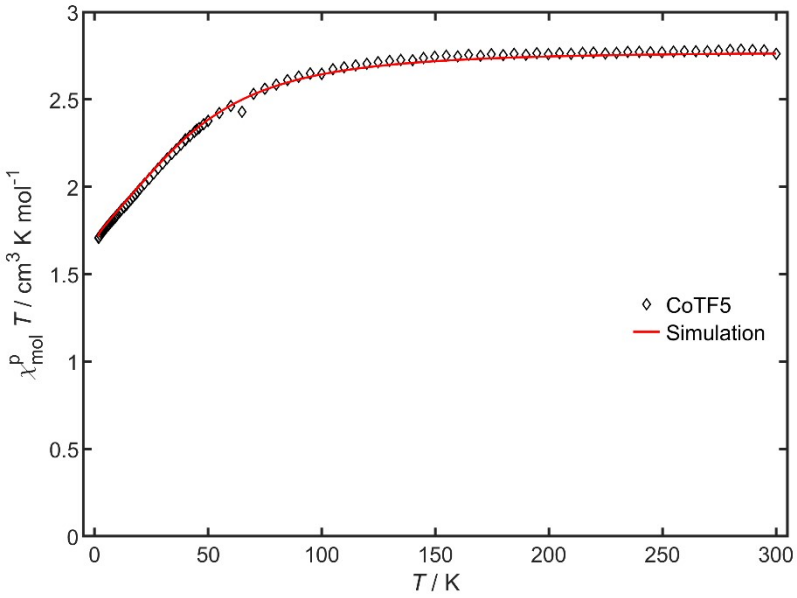

Figure S3.1: Susceptibility temperature product as a function of the temperature of **CoTF5**, immobilized in eicosane as well as the corresponding spin Hamiltonian simulation. The parameters of the simulation are shown in table 5. The simulation is shown as a red straight line.

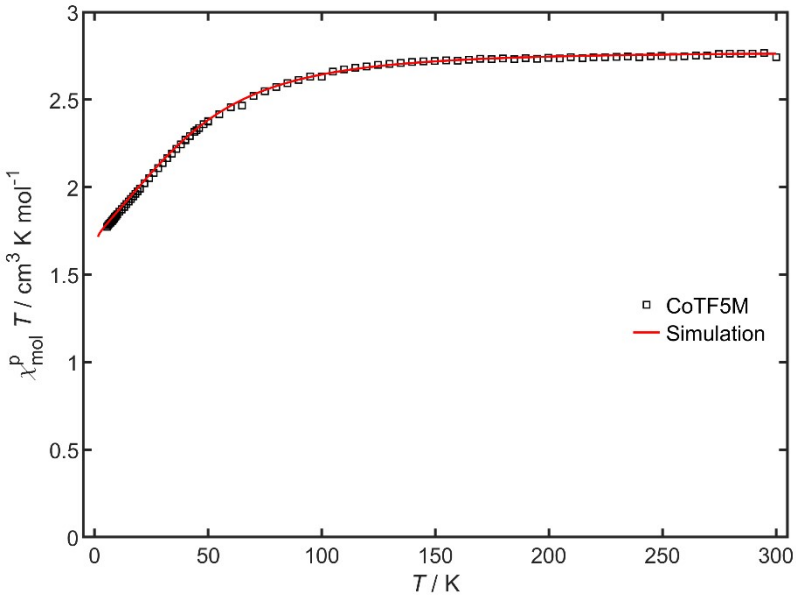

Figure S3.2: Susceptibility temperature product as a function of the temperature of **CoTFM**, immobilized in eicosane as well as the corresponding spin Hamiltonian simulation. The parameters of the simulation are shown in table 5. The simulation is shown as a red straight line.

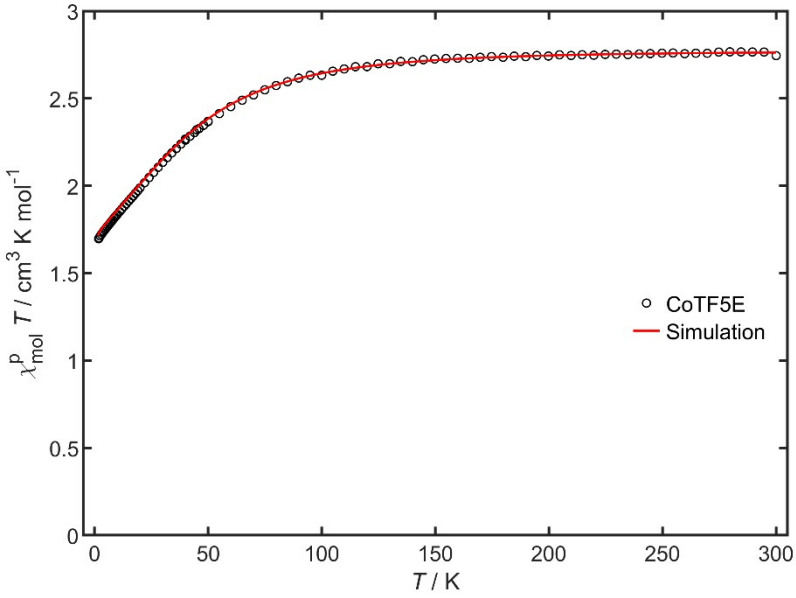

Figure S3.3: Susceptibility temperature product as a function of the temperature of **CoTF5E**, immobilized in eicosane as well as the corresponding spin Hamiltonian simulation. The parameters of the simulation are shown in table 5. The simulation is shown as a red straight line.

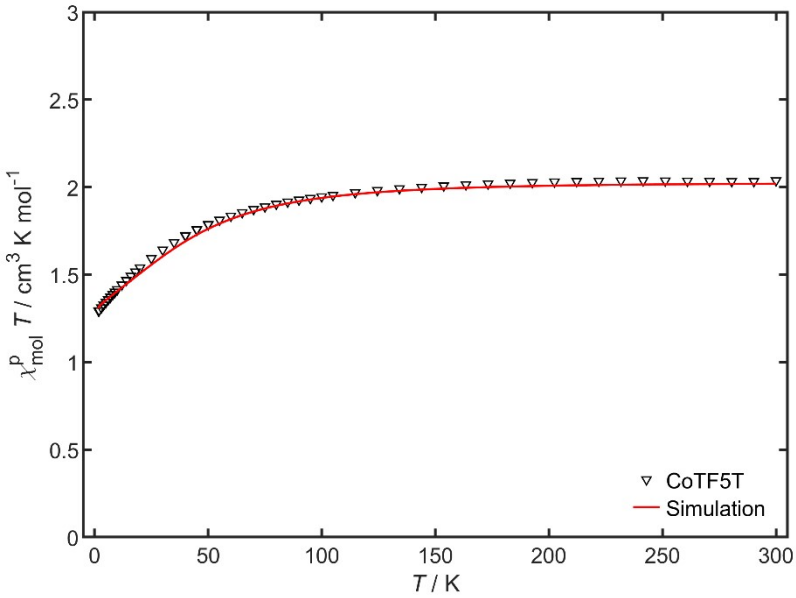

Figure S3.4: Susceptibility temperature product as a function of the temperature of **CoTF5T**, immobilized in eicosane as well as the corresponding spin Hamiltonian simulation. The parameters of the simulation are shown in table 5. The simulation is shown as a red straight line.

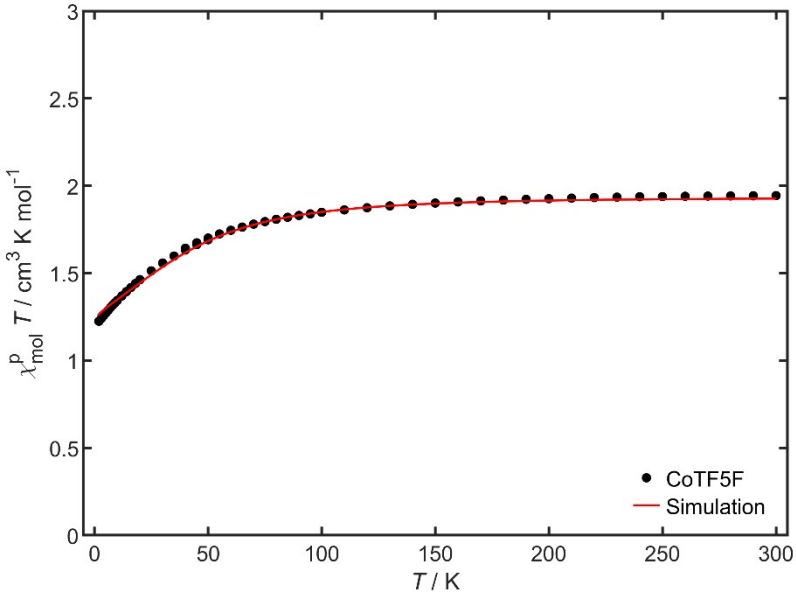

Figure S3.5: Susceptibility temperature product as a function of the temperature of **CoTF5F**, immobilized in eicosane as well as the corresponding spin Hamiltonian simulation. The parameters of the simulation are shown in table 5. The simulation is shown as a red straight line.

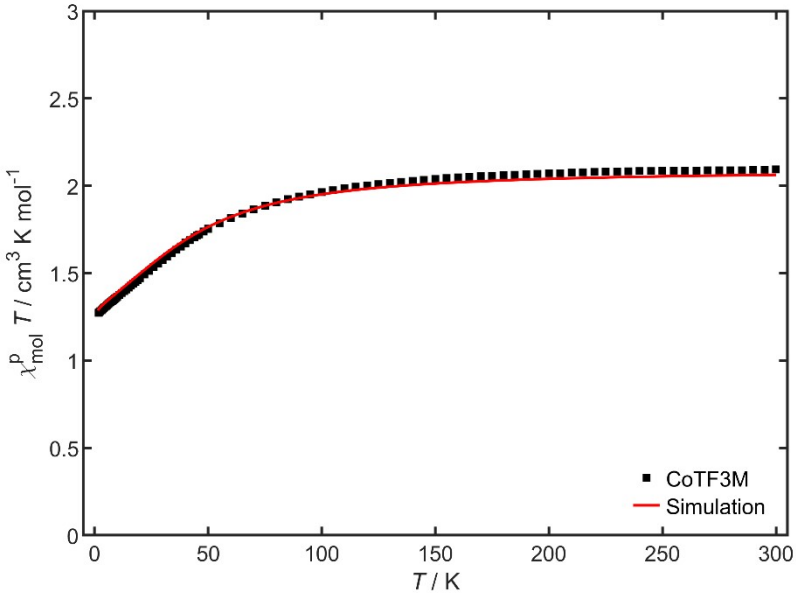

Figure S3.6: Susceptibility temperature product as a function of the temperature of **CoTF3M**, immobilized in eicosane as well as the corresponding spin Hamiltonian simulation. The parameters of the simulation are shown in table 5. The simulation is shown as a red straight line.

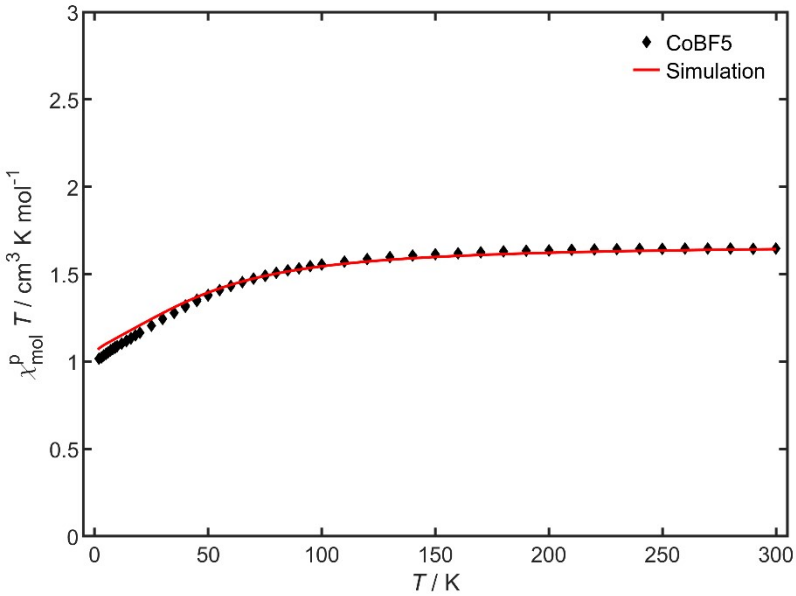

Figure S3.7: Susceptibility temperature product as a function of the temperature of **CoBF5**, immobilized in eicosane as well as the corresponding spin Hamiltonian simulation. The parameters of the simulation are shown in table 5. The simulation is shown as a red straight line.

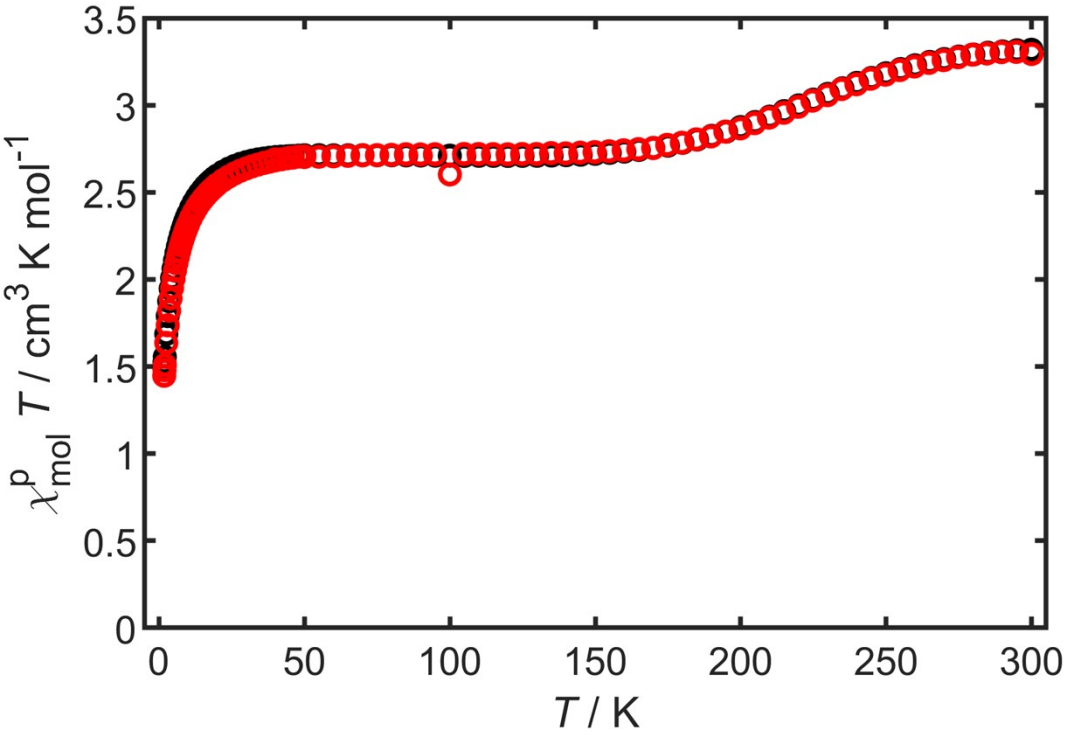

Figure S4: Susceptibility temperature product as a function of the temperature of **FeTF5E**, when pressed into a pellet. A partial loss of the SCO properties is observed, when the compound is pressed into a pellet.

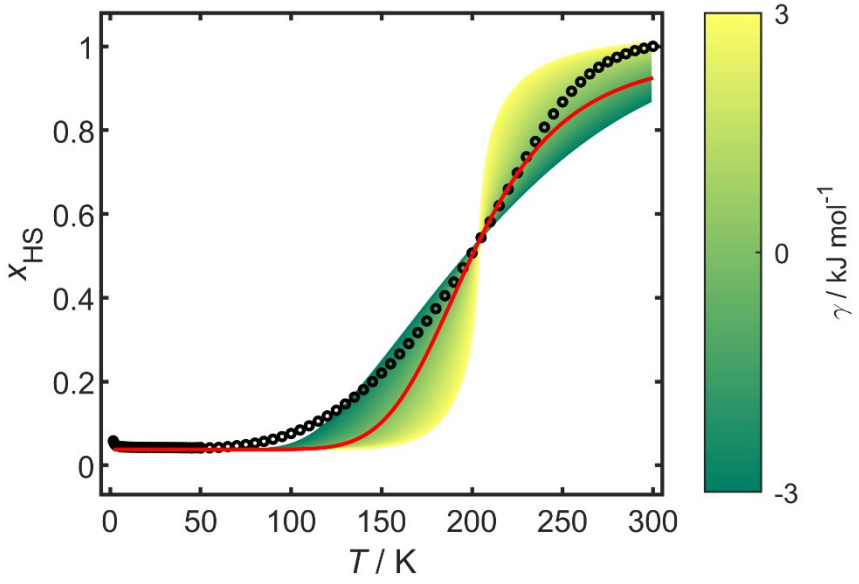

Figure S5: Fit of the experimental HS molar fraction obtained by SQUID magnetometry (black circles) on the basis of the Slichter-Drickamer model with the cooperativity Γ = 0 kJ mol^{-1} and the thermodynamic parameters ΔH = 12.7(8) kJ mol^{-1} and ΔS = 63(4) JK^{-1}mol^{-1} (red line). Other lines (green to yellow) represent simulations with the same values for ΔH and ΔS as in the red line but varying cooperativity Γ as indicated in the color bar.

HFEPR Measurements

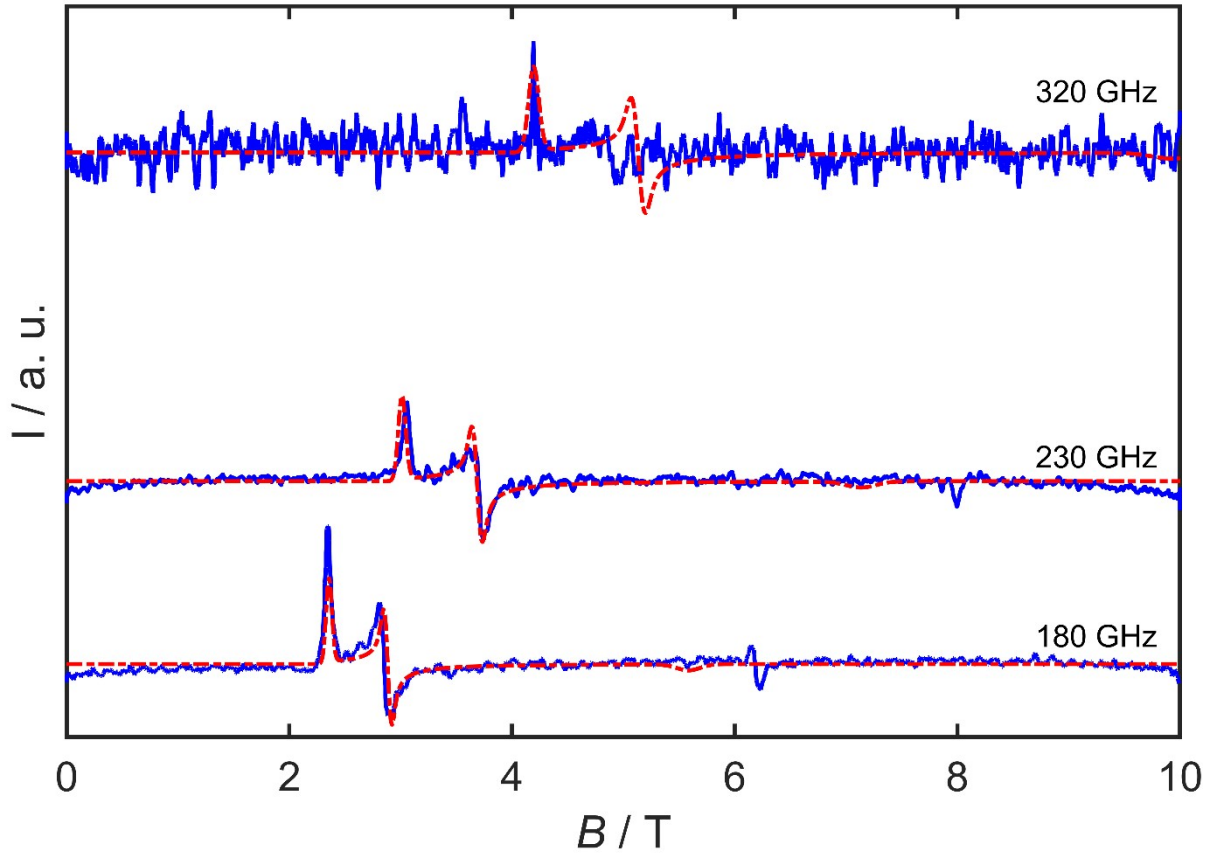

Figure S6: HFEPR measurement of **CoTF5** (blue) at 180, 230 and 320 GHz as well as the corresponding simulations (red dashed line). Simulation parameters are found in Table 5.

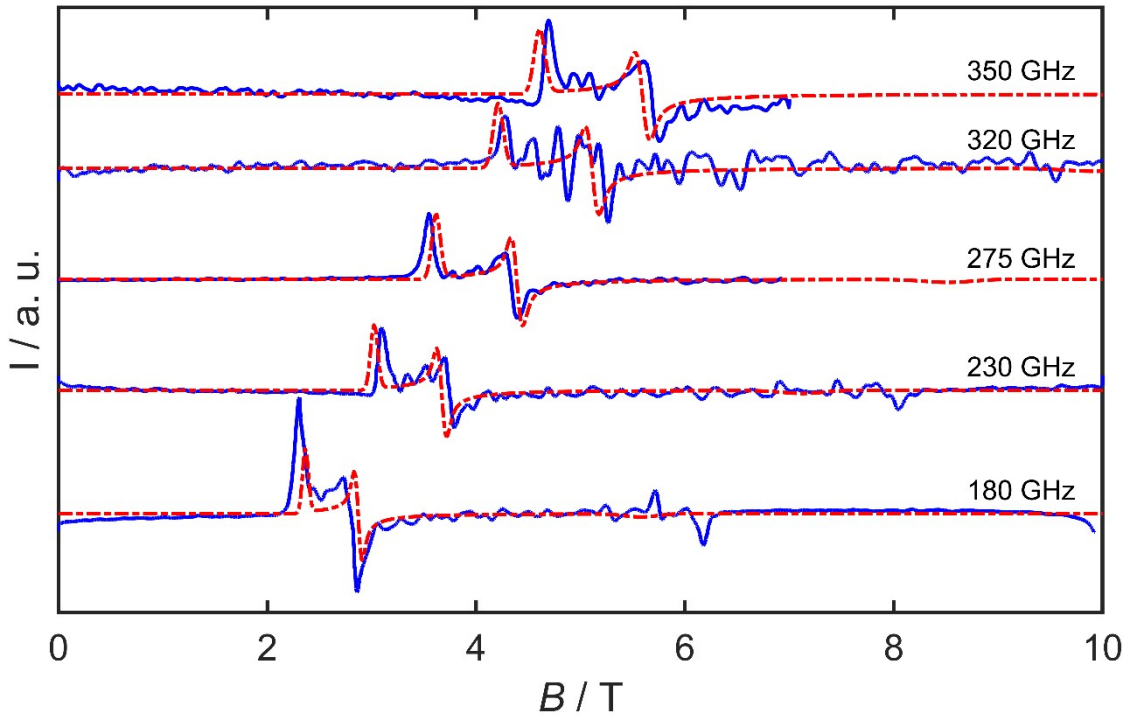

Figure S7: HFEPR measurement of **CoTF5M** (blue) at 180, 230, 275, 320 and 350 GHz as well as the corresponding simulations (red dashed line). Simulation parameters are found in Table 5.

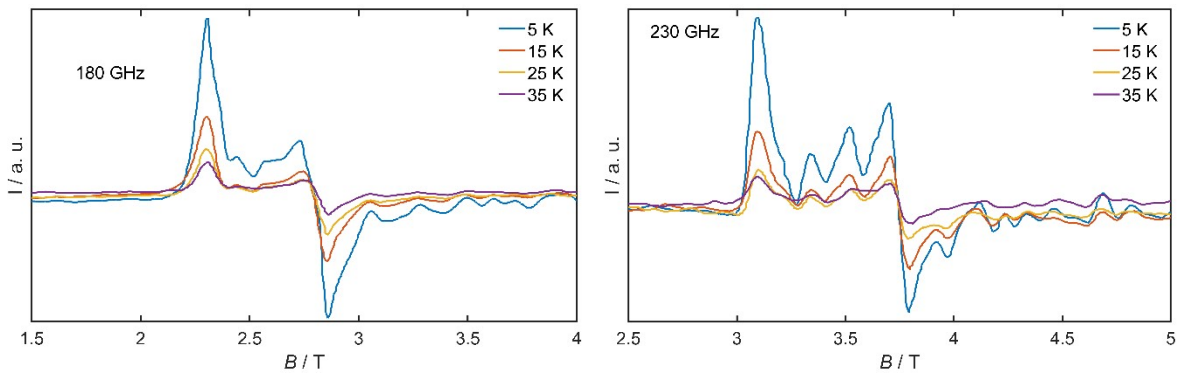

Figure S8: HFEPR measurement of **CoTF5M** at different temperatures. The frequency of each measurement set is shown in the figure.

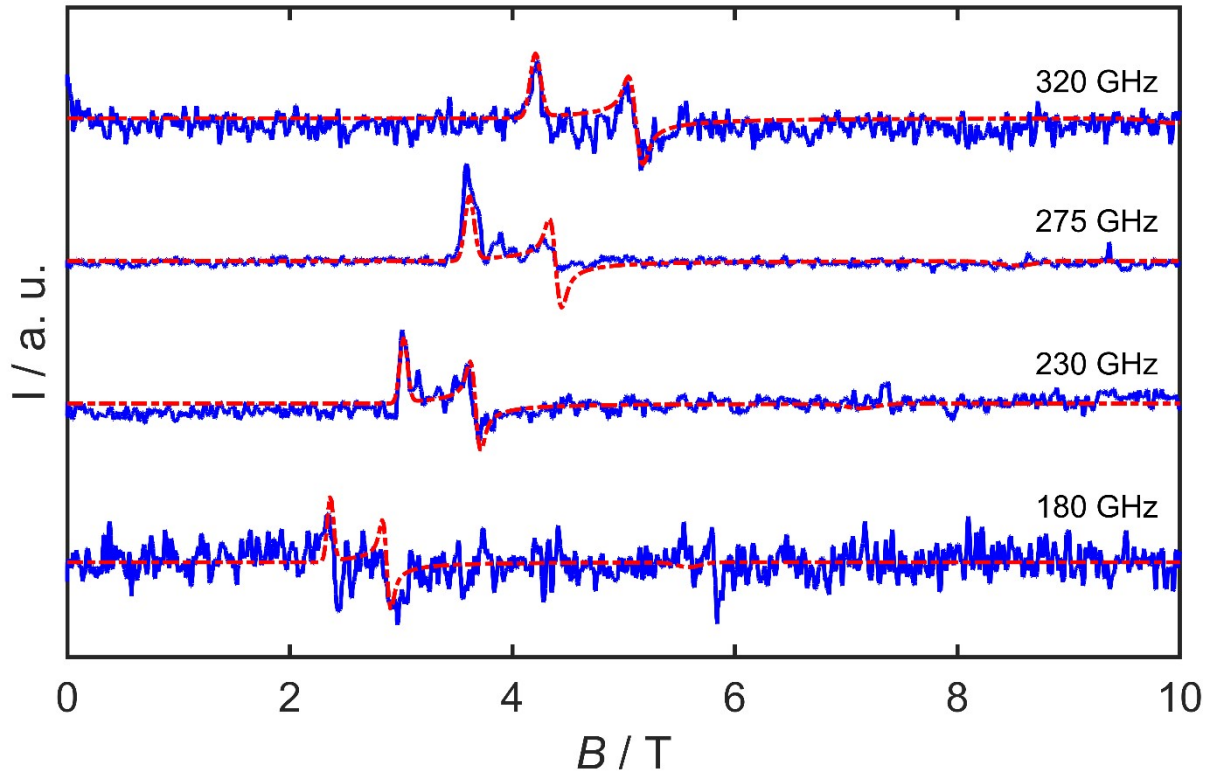

Figure S9: HFEPR measurement of **CoTF5E** (blue) at 180, 230, 275 and 320 GHz as well as the corresponding simulations (red dashed line). Simulation parameters are found in Table 5.

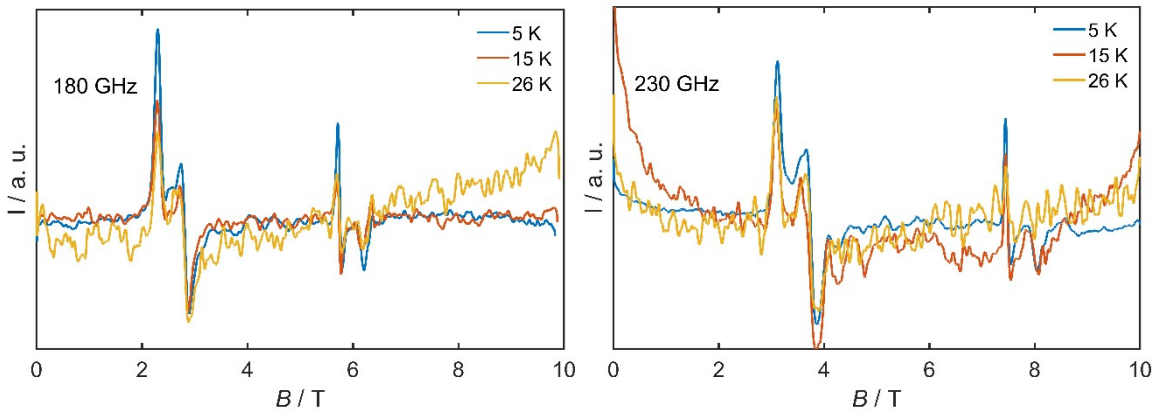

Figure S10: HFEPR measurement of **FeTF5E** at different temperatures. The corresponding frequencies are shown in the figure.

Mössbauer Spectroscopy

Table S1: Overview of the fit parameters from the temperature dependent Mössbauer measurements of **FeTF5E**.

System		85 K	120 K	170 K	214 K	240 K	293 K
$S = 2$	δ / mm s^{-1}	-	-	1.13(1)	1.01(1)	1.00(1)	0.94(1)
	ΔE_Q / mm s^{-1}	-	-	1.58(1)	1.26(2)	1.26(1)	1.13(1)
	Γ / mm s^{-1}	-	-	0.29(1)	0.46(1)	0.52(1)	0.39(1)
$S = 0$	δ / mm s^{-1}	0.57(1)	0.54(1)	0.55(1)	0.55(1)	0.55(1)	-
	ΔE_Q / mm s^{-1}	0.66(1)	0.70(1)	0.66(1)	0.66(1)	0.66(1)	-
	Γ / mm s^{-1}	0.30(1)	0.34(1)	0.36(1)	0.36(1)	0.40(1)	-
	HS molar fraction	0	0	0.12	0.41	0.63	1

UV/Vis Spectroscopy

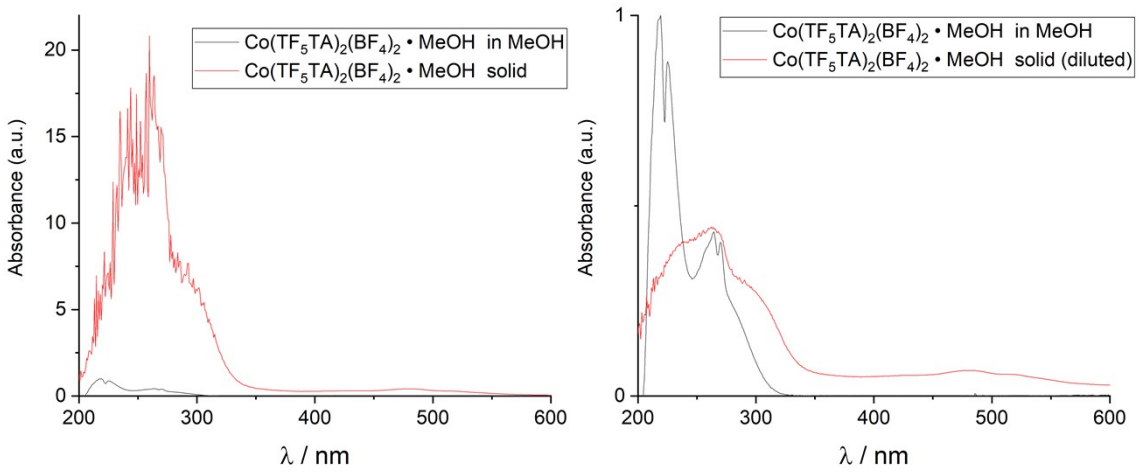

Figure S11: UV/Vis spectra of **CoTF5M**.

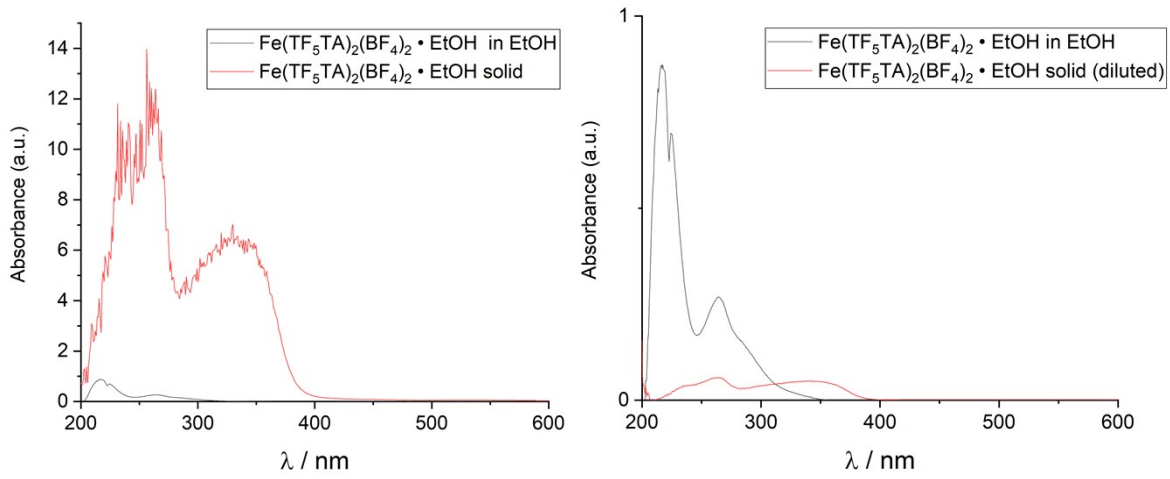

Figure S12: UV/Vis spectra of **FeTF5E**.

IR Spectroscopy

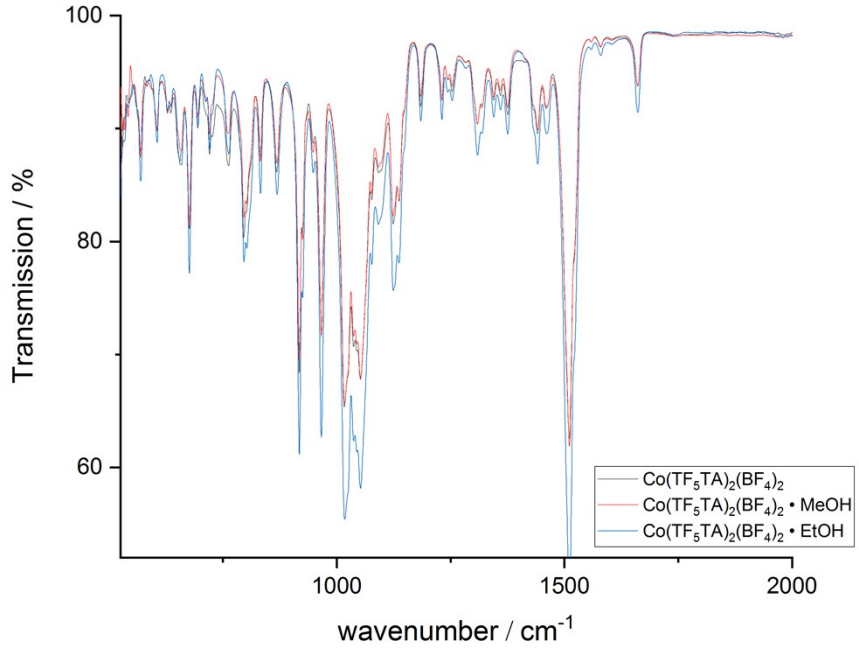

Figure S13: IR spectra of $Co(TF_5TA)_2(BF_4)_2$ complexes **CoTF5-CoTF5E**.

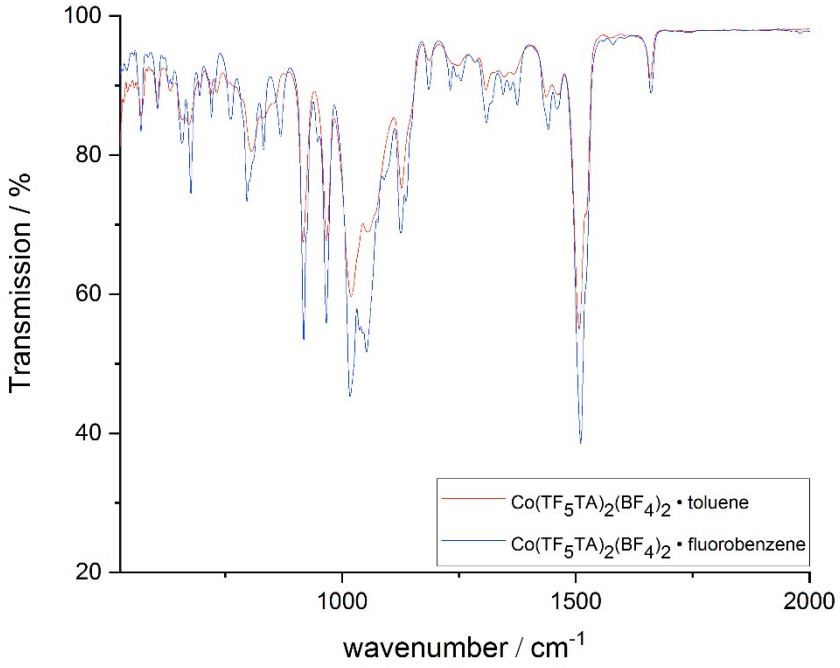

Figure S14: IR spectra of $Co(TF_5TA)_2(BF_4)_2$ complexes **CoTF5T** and **CoTF5F**.

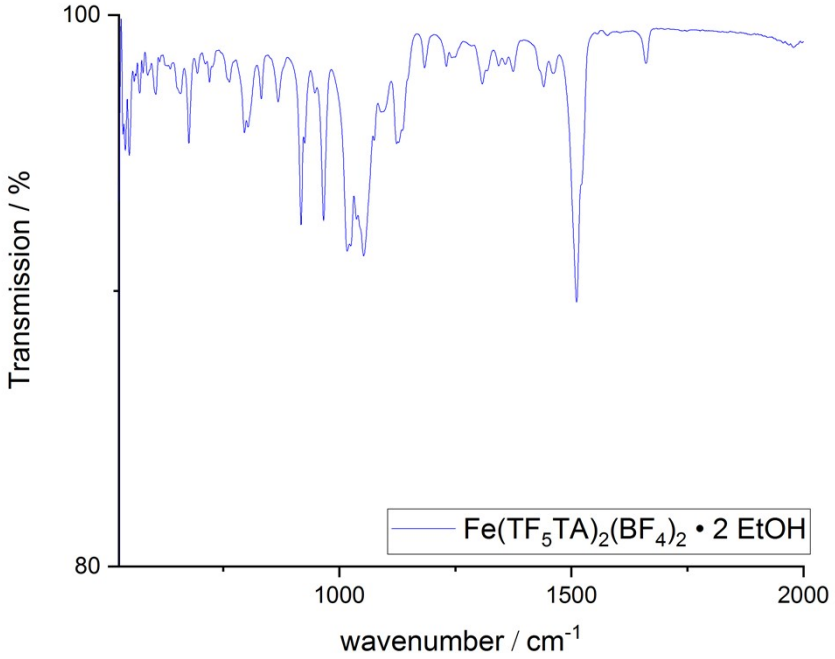

Figure S15: IR spectra of $Fe(TF_5TA)_2(BF_4)_2 \cdot 2$ EtOH **FeTF5E**.

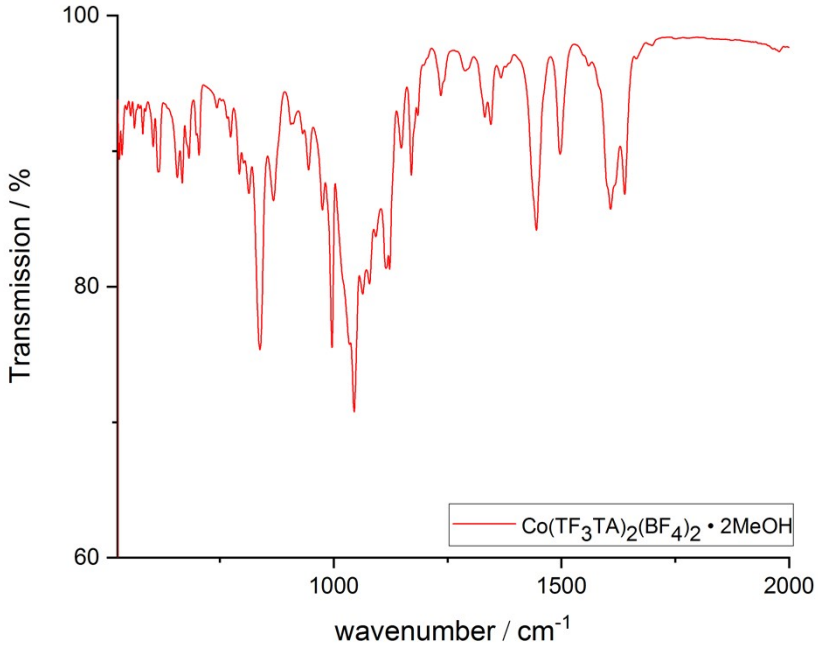

Figure S16: IR spectra of $Co(TF_3TA)_2(BF_4)_2 \cdot 2$ MeOH **CoTF3M.**

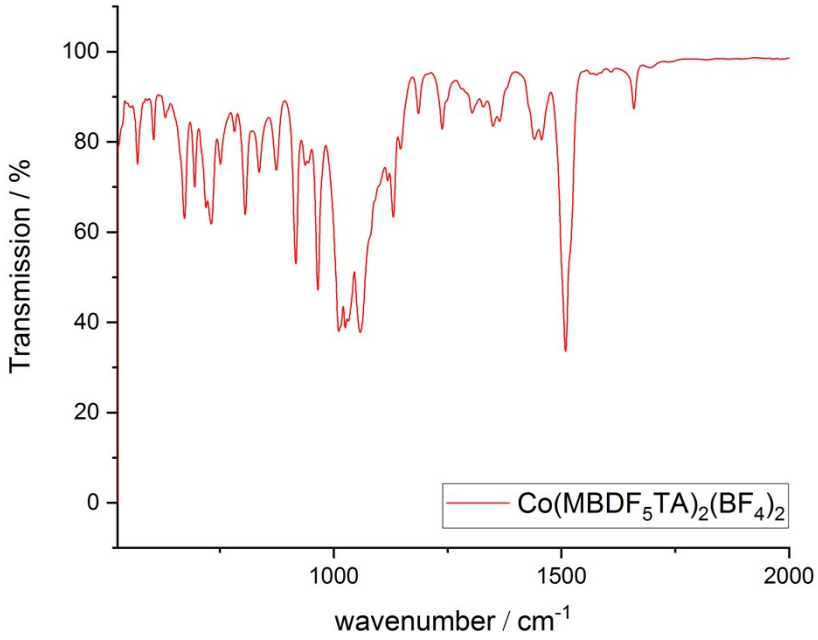

Figure S17: IR spectra of $Co(MBDF_5TA)_2(BF_4)_2$ **CoBF5**.

X-Ray Crystallography

Table S2: Crystallographic data of **CoTF5**, **CoTF5M** and **CoTF5E**.

	CoTF5	**CoTF5M**	**CoTF5E**
Chemical formula	$C_{62}H_{35}B_2CoF_{38}N_{20}O$	$C_{60}H_{30}B_2CoF_{38}N_{20}$	$C_{62}H_{62}B_2CoF_{14}N_{20}O_2$
M_r	1878.65	1833.59	1465.86
Crystal system	*Monoclinic*	*Monoclinic*	*Monoclinic*
Space group	$P2_1/n$	$P2_1/n$	$P2_1/n$
a (Å)	15.993(8)	15.8479(11)	7.7391(3)
b (Å)	9.445(5)	9.3920(8)	20.7813(8)
c (Å)	24.337(11)	24.1324(19)	20.1509(9)
α(°)	90	90	90
β (°)	105.061(10)	104.601(3)	98.408(3)
γ (°)	90	90	90
V (Å^3)	3550(3)	3474.9(5)	3206.0(2)
Z	2	2	2
Densitiy (g cm^{-3})	1.757	1.752	1.518
F(000)	1868	1818	1506
Radiation Type	MoK_α	MoK_α	CuK_α
μ (mm^{-1})	0.402	0.407	3.003
Crystal size	0.380 x 0.070 x 0.040	0.43 x 0.12 x .0.8	0.18x0.08x0.08
Meas. Refl.	46191	48490	21514
Indep. Refl.	7290	7969	5786
Obsvd. [$I > 2\sigma(I)$] refl.	5713	6355	4420
R_{int}	0.0538	0.0405	0.0634
R [$F^2 > 2\sigma(F^2)$], wR(F^2), S	0.0574, 0.1435, 1.010	0.0373, 0.0882, 1.036	0.0928, 0.2274, 1.094
$\Delta\rho_{max}$, $\Delta\rho_{min}$ (e Å^{-3})	1.084, -0.554	0.295, -0.298	0.882, -0.660
cif	bip333_a	bip521_a	bip322_a

Table S3: Crystallographic data of **CoTF5T**, **CoTF5F** and **FeTF5E**.

	CoTF5T	**CoTF5F**	**FeTF5E**
Chemical formula	$C_{72.05}H_{46}B_2CoF_{38}N_{20}O_{0.65}$	$C_{142}H_{85}B_4Co2F_{79}N_{40}O$	$C_{60}H_{30}B_2F_{38}FeN_{20}$
M_r	2004.823	4029.59	1830.51
Crystal system	*Triclinic*	*Triclinic*	*Monoclinic*
Space group	*P*-1	*P*-1	$P2_1/n$
a (Å)	11.698(1)	11.735(1)	16.2429(9)

b (Å)	18.925(1)	18.920(2)	9.3972(5)
c (Å)	19.405(1)	19.260(2)	24.0242(12)
α(°)	68.616(2)	68.474(4)	90
β (°)	80.878(3)	80.359(3)	105.545(2)
γ (°)	86.182(3)	86.509(3)	90
V (Å^3)	3949.9(5)	3921.8(7)	3532.9(3)
Z	2	1	2
Densitiy (g cm^{-3})	1.686	1.706	1.721
F(000)	2007.473	2010	1816
Radiation Type	MoK_α	MoK_α	MoK_α
μ (mm^{-1})	0.367	0.373	0.371
Crystal size	0.44, 0.33, 0.11	0.27, 0.17, 0.08	0.16, 0.08, 0.08
Meas. Refl.	72484	104728	40698
Indep. Refl.	16211	14271	6497
Obsvd. [$I > 2\sigma(I)$] refl.	11515	10992	4691
R_{int}	0.0737	0.0712	0.0872
R [$F^2 > 2\sigma(F^2)$], wR(F^2), S	0.0650, 0.1598, 1.0734	0.0490, 0.1236, 1.039	0.0640, 0.2179, 0.710
$\Delta\rho_{max}$, $\Delta\rho_{min}$ (e Å^{-3})	1.5601, -0.9186	0.971, -0.856	0.661, -0.860
cif	bip226_a	bip576_2_a	bip522_a

Table S4: Crystallographic data of **CoTF3M** and **CoBF5**.

	CoTF3M	**CoBF5**
Chemical formula	$C_{62}H_{50}B_2CoF_{26}N_{20}O_2$	$C_{60}H_{41.62}B_{1.96}CoF_{27.95}N_{20}$
M_r	1681.77	1653.90
Crystal system	*Monoclinic*	*Monoclinic*
Space group	*I*2/*a*	*C*2/*c*
a (Å)	11.9249(1)	24.6532(5)
b (Å)	25.4211(2)	24.4358(5)
c (Å)	23.3641(2)	11.6193(2)
α(°)	90	90
β (°)	99.6857(8)	105.695(1)
γ (°)	90	90
V (Å^3)	6981.7(1)	6738.7(2)

Z	4	4
Densitiy (g cm^{-3})	1.600	1.630
F(000)	3396	3320
Radiation Type	CuK_α	MoK_α
μ (mm^{-1})	3.100	0.390
Crystal size	0.12, 0.07, 0.04	0.45, 0.33, 0.32
Meas. Refl.	38755	50937
Indep. Refl.	6686	6157
Obsvd. [$I > 2\sigma(I)$] refl.	5988	5704
R_{int}	0.0253	0.0269
R [$F^2 > 2\sigma(F^2)$], wR(F^2), S	0.0408, 0.1122, 1.052	0.0598, 0.1647, 1.213
$\Delta\rho_{max}$, $\Delta\rho_{min}$ (e $Å^{-3}$)	0.346, -0.233	1.057, -0.461
cif	Co_L2_100K_Cu	bip587_a

Computational Details

All SCS-MP2 calculations were performed using the TURBOMOLE program package, version 7.4.1.[15-17]

Structures were optimized at the SCS-MP2 level of theory using the aug-cc-pVTZ basis set[18] for all atoms and the corresponding auxiliary basis sets.[19, 20] To correct for basis set superposition errors, the counterpoise correction was applied for both energy calculations and during the structure optimization. SCF was converged to energy changes below 10^{-8} a.u., structures were optimized to a largest Cartesian gradient component below 10^{-4} a.u. All optimizations used the larges possible point group symmetry.

Energies were calculated at the SCS-MP2-F12 level of theory using cc-pVTZ-F12 basis sets[21] and the corresponding auxiliary basis sets[22, 23] and employing C_1 symmetry. Coupled Cluster corrections to these energies were calculated at the CCSD(T) level of theory using the aug-cc-pVDZ basis set.

Additional energies were calculated at the DLPNO-CCSD(T)-F12 level of theory using the ORCA program package, version 4.2.0.[24] Both sets of energies are given in table S5. All energies agree with the energies obtained at the SCS-MP2-F12/cc-pVTZ-F12 level of theory (see main text, table 3) up to 2 kJ mol^{-1}.

Table S5: Calculated interaction energies of the different dimer structures optimized at the SCS-MP2/aug-cc-pVTZ (CP corrected) level of theory.

(I)	S	PD	T	TT
$C_6H_6 \cdots C_6H_6$	-6.9	-11.2	-11.2	-10.0
$C_6F_6 \cdots C_6F_6$	-13.8	-19.1	-7.9	-9.7
$C_6H_6 \cdots C_6F_6$	-23.4	-25.0	-8.0/-4.4	-7.7/-5.1
(II)				
$C_6H_6 \cdots C_6H_6$	-6.1	-9.8	-11.1	-9.7
$C_6F_6 \cdots C_6F_6$	-14.5	-19.2	-7.9	-9.7
$C_6H_6 \cdots C_6F_6$	-22.0	-23.4	-8.4/-4.6	-8.2/-5.2

Energies (I): SCS-MP2-F12/cc-pVTZ-F12 + $\Delta_{CCSD(T)}$(aug-cc-pVDZ) (CP corrected) [kJ mol^{-1}]
Energies(II): DLPNO-CCSD(T)-F12/cc-pVTZ-F12 (CP corrected) [kJ mol^{-1}]

Additional calculations on higher oligomers were performed at the DFT level of theory using the PBE0 functional[25] and the def2-QZVPP basis set.[26] All calculations employed the RIJ approximation and Grimme's empirical D4 dispersion correction[27] This setup was shown to reproduce the results of CP-SCS-MP2/aug-cc-pVTZ up to 2 kJ mol^{-1}in relative energies and 2.4 pm in structural parameters, respectively. The results of these calculations are shown in Table S6.

Table S6: Calculated interaction energies of the different oligomeric structures at RI-PBE0-D4/def2-QZVPP (energies in kJ mol^{-1}) level of theory. With a mean absolute error for dimers compared to CP-SCS-MP2: 1.6 kJ mol^{-1} in energies and 2.4 pm in structures.

Parallel Layers (C_{2h})	n = 2	n = 3	n = 4	n = 5
$(C_6H_6)_n$	-13.0	-26.0	-39.1	-52.1
$(C_6F_6)_n$	-22.1	-44.3	-66.6	-88.8
Closer Packing	n = 2 (C_{2h})	n = 3 (C_{3h})	n = 4 (S_4)	n = 5 (C_1)
$(C_6H_6)_n$	-13.0	-33.2	-62.8	-82.5
$(C_6F_6)_n$	-22.1	-33.6	-60.1	-93.2

NMR Spectra

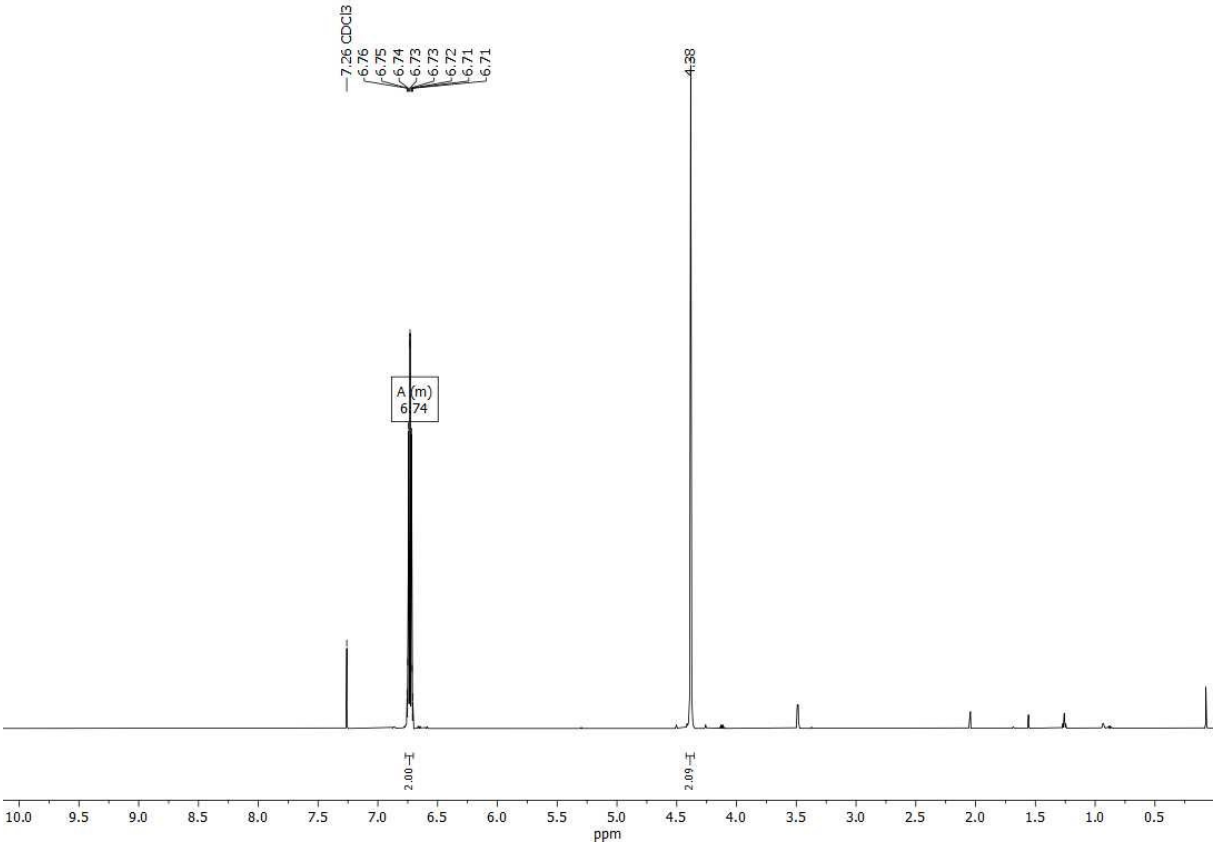

Figure S18: ^{1}H NMR of trifluorobenzylazide in $CDCl_3$.

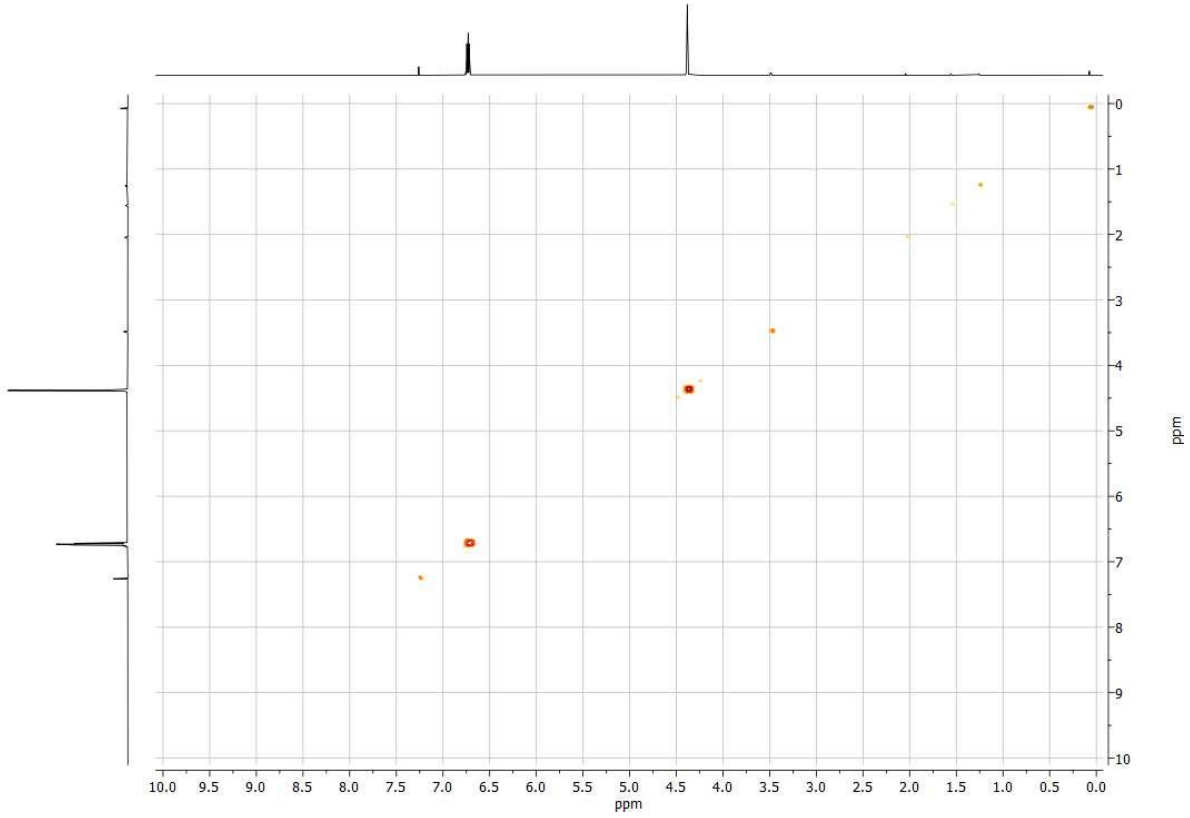

Figure S19: ^{1}H ^{1}H COSY NMR of trifluorobenzylazide in $CDCl_3$.

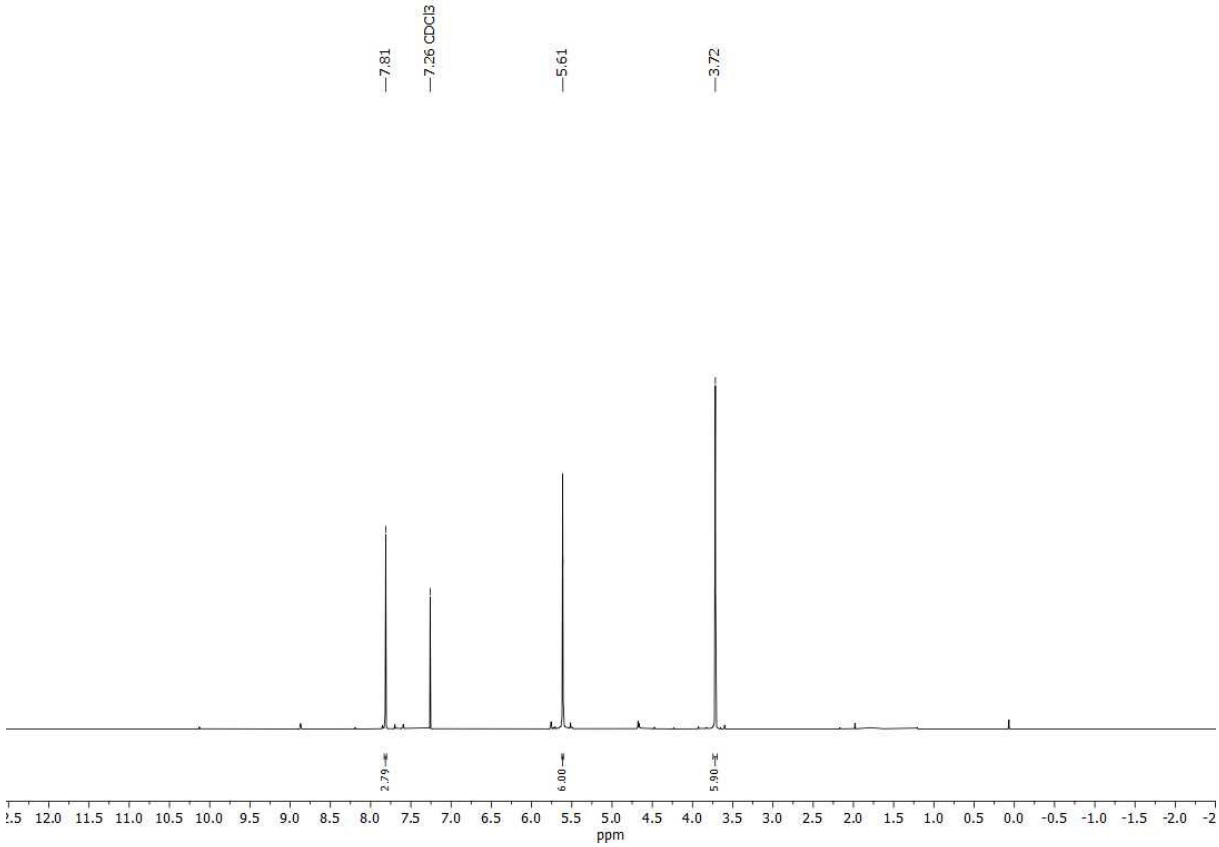

Figure S20: ^{1}H NMR of TF_5TA in $CDCl_3$.

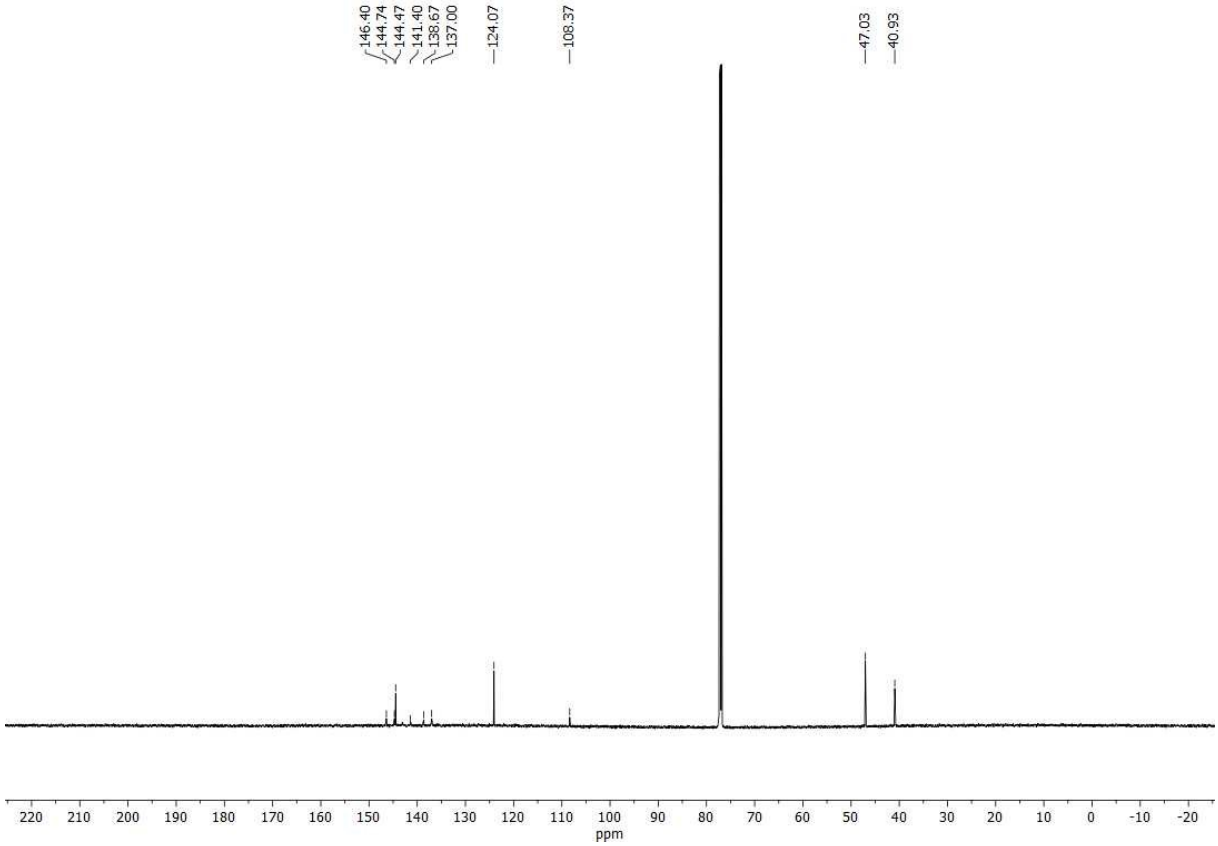

Figure S21: ^{13}C NMR of TF_5TA in $CDCl_3$.

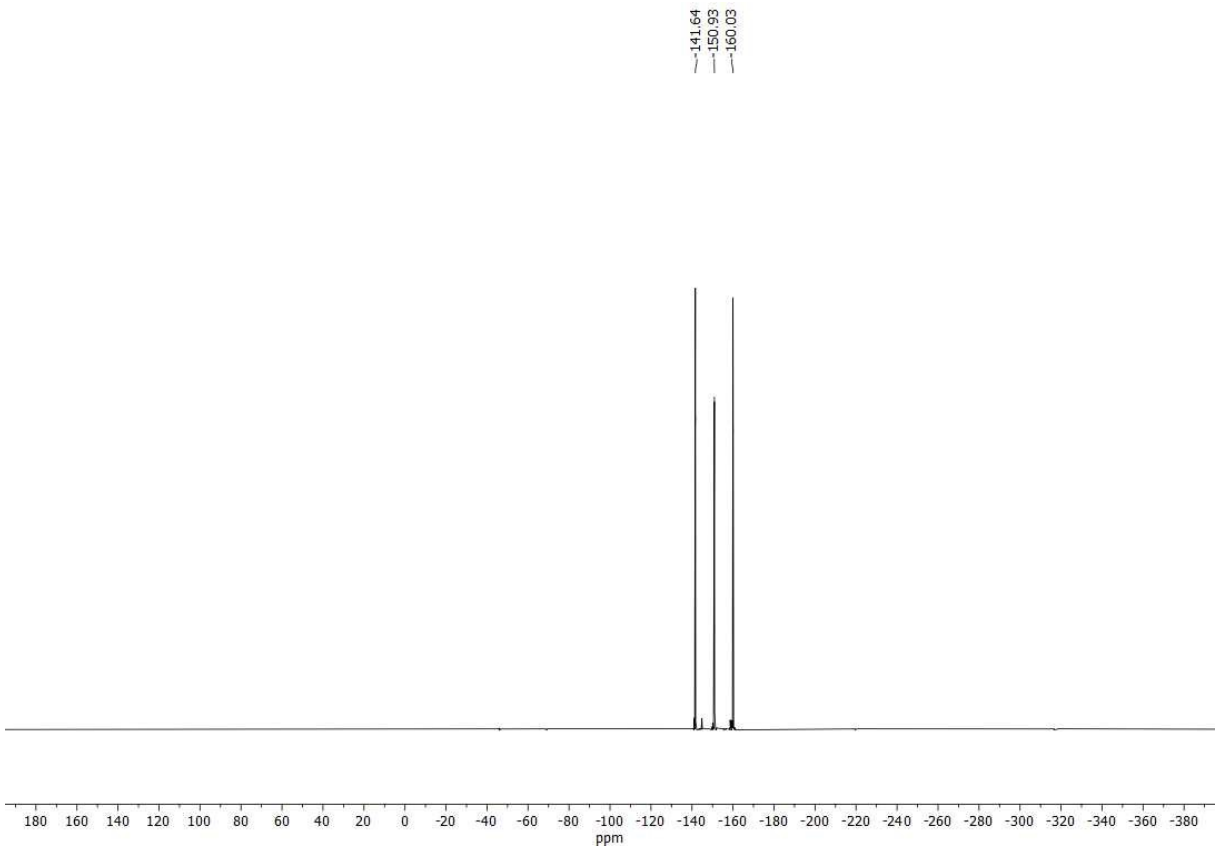

Figure S22: ^{19}F NMR of TF_5TA in $CDCl_3$.

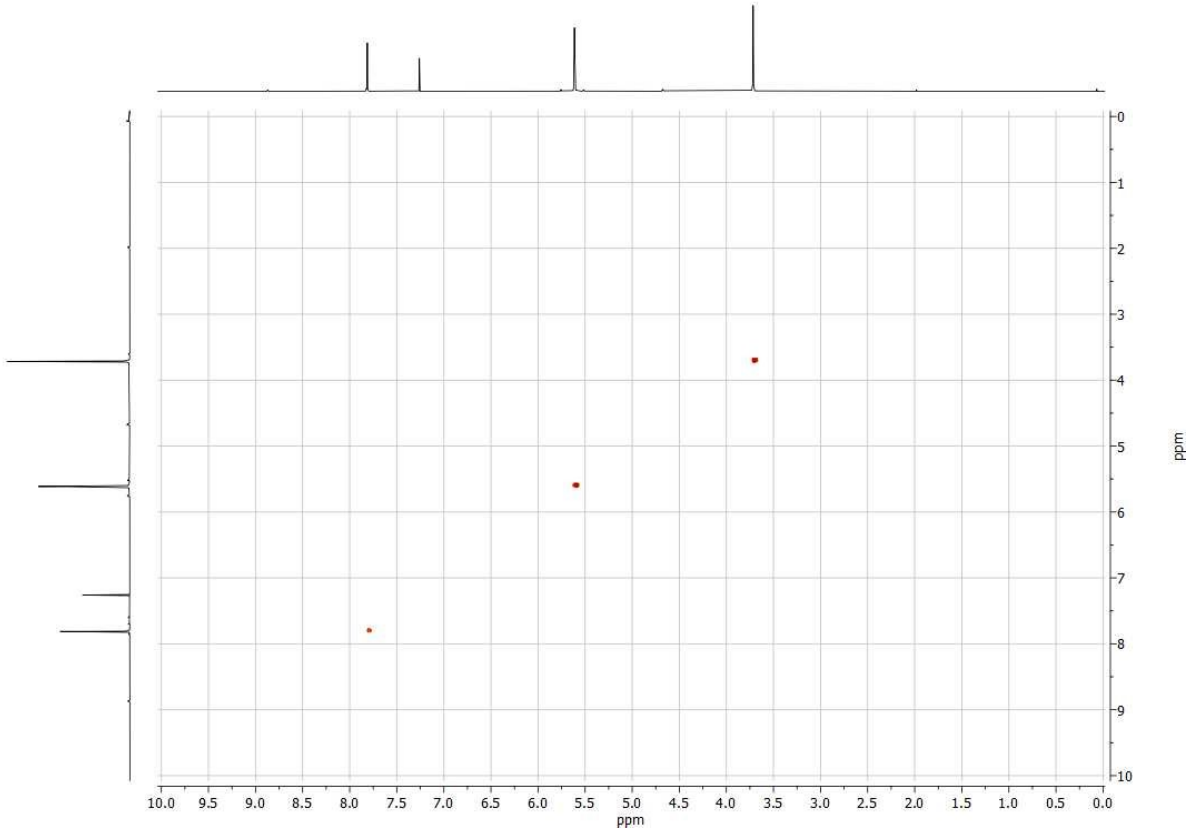

Figure S23: ^{1}H ^{1}H COSY NMR of TF_5TA in $CDCl_3$.

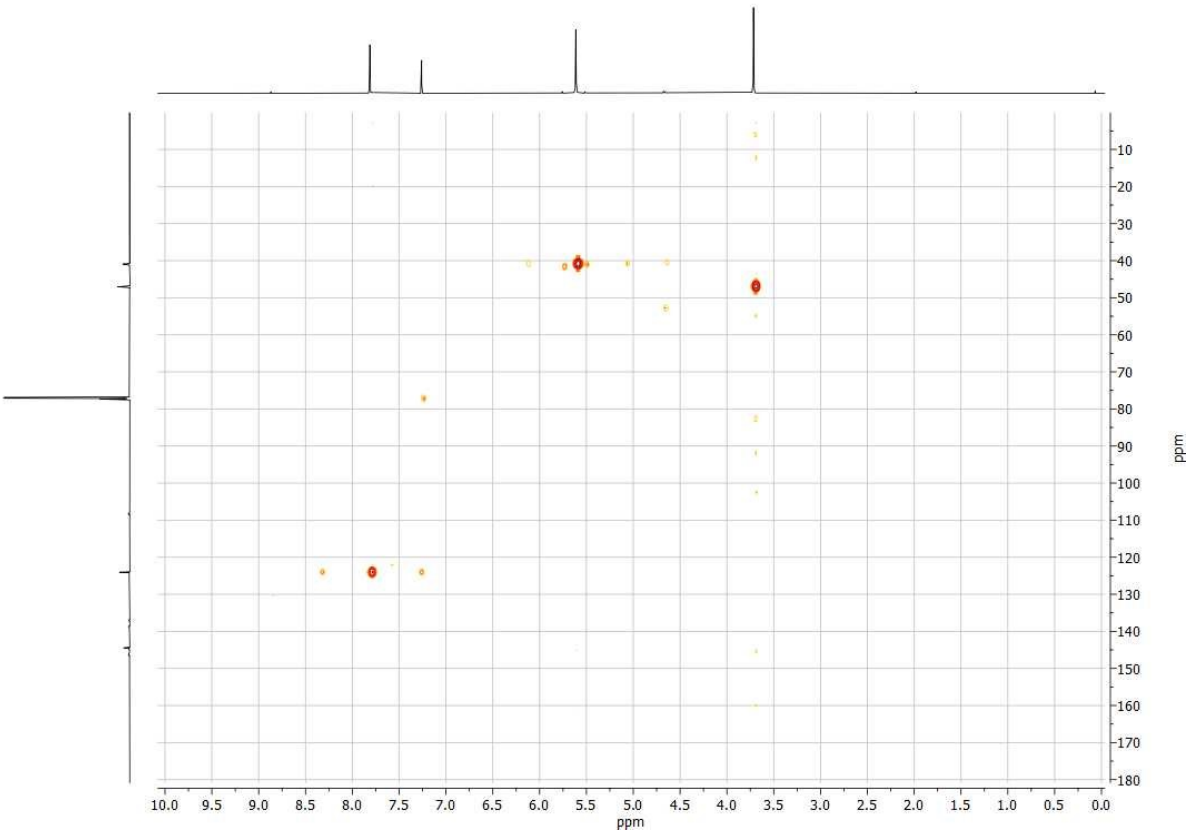

Figure S24: ^{1}H ^{13}C HMBC NMR of TF_5TA in $CDCl_3$.

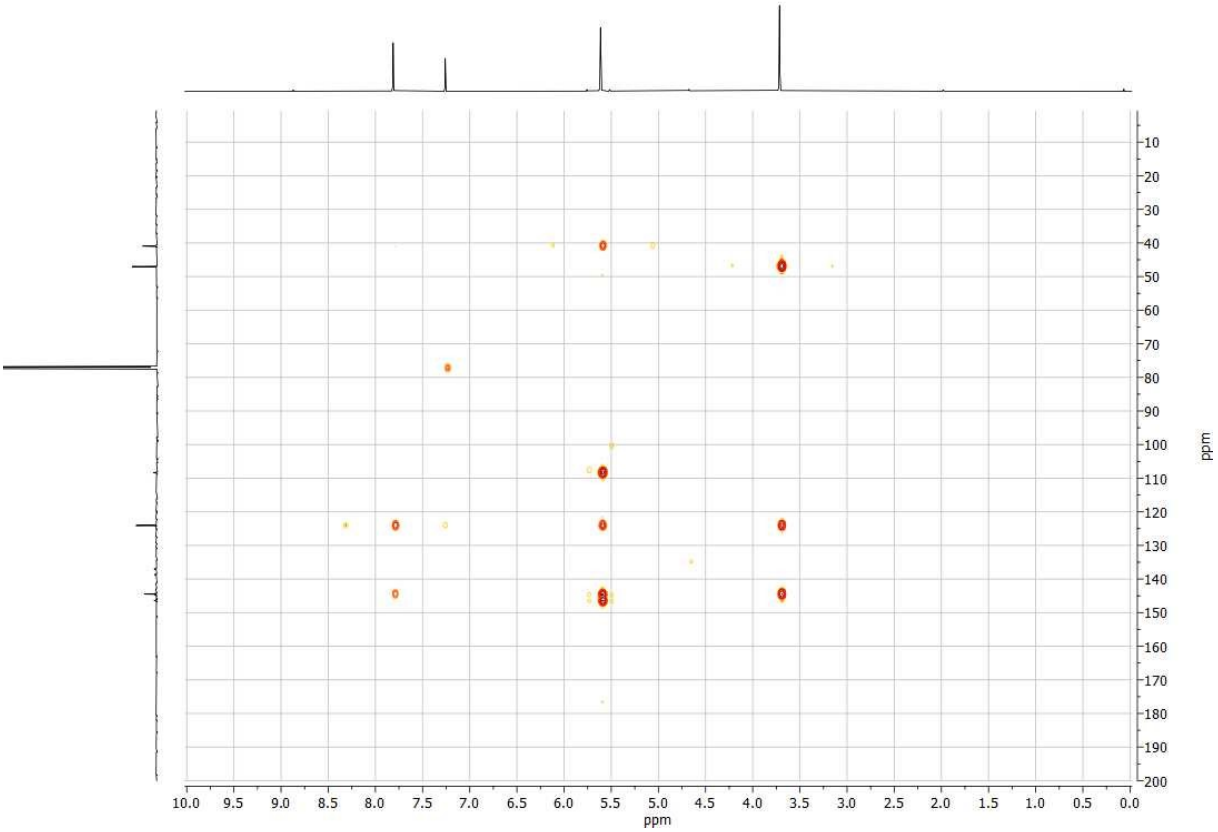

Figure S25: ^{1}H ^{13}C HMQC NMR of TF_5TA in $CDCl_3$.

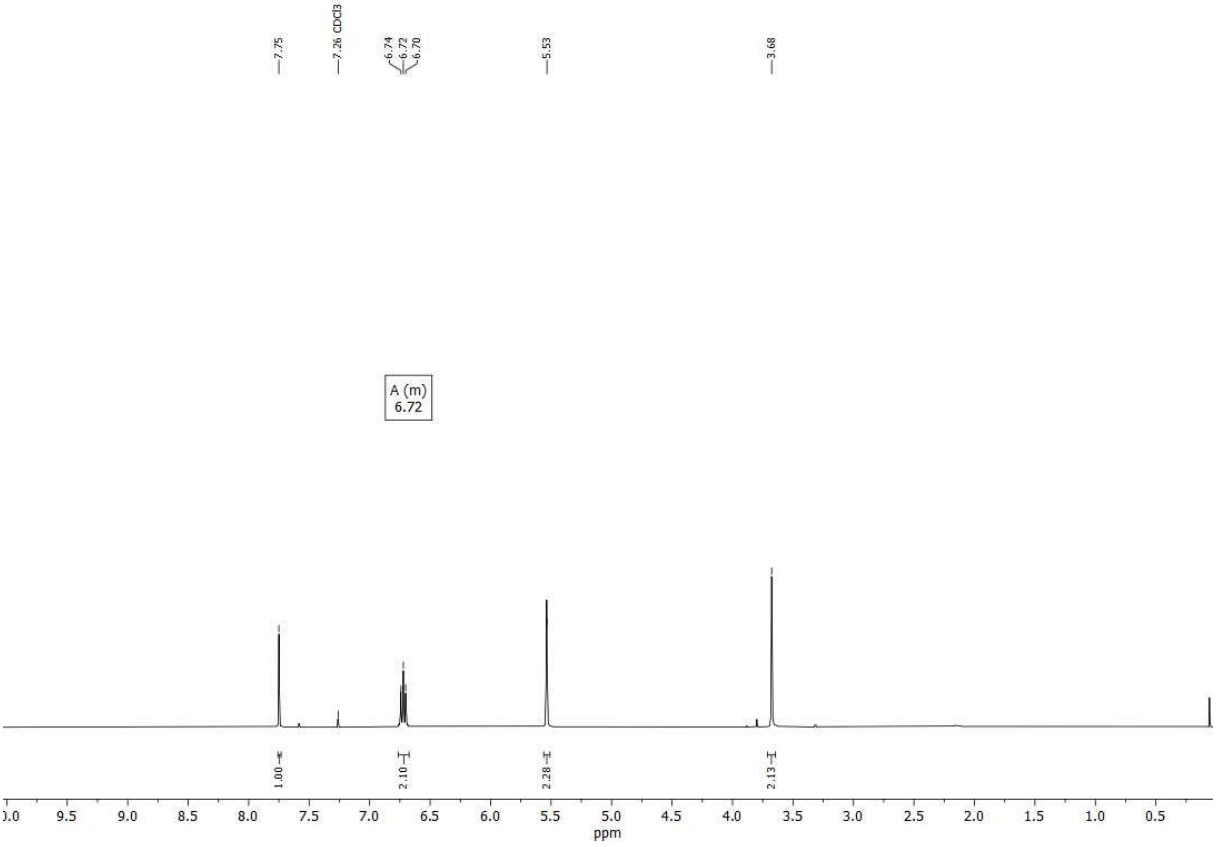

Figure S26: ^{1}H NMR of TF_3TA in $CDCl_3$.

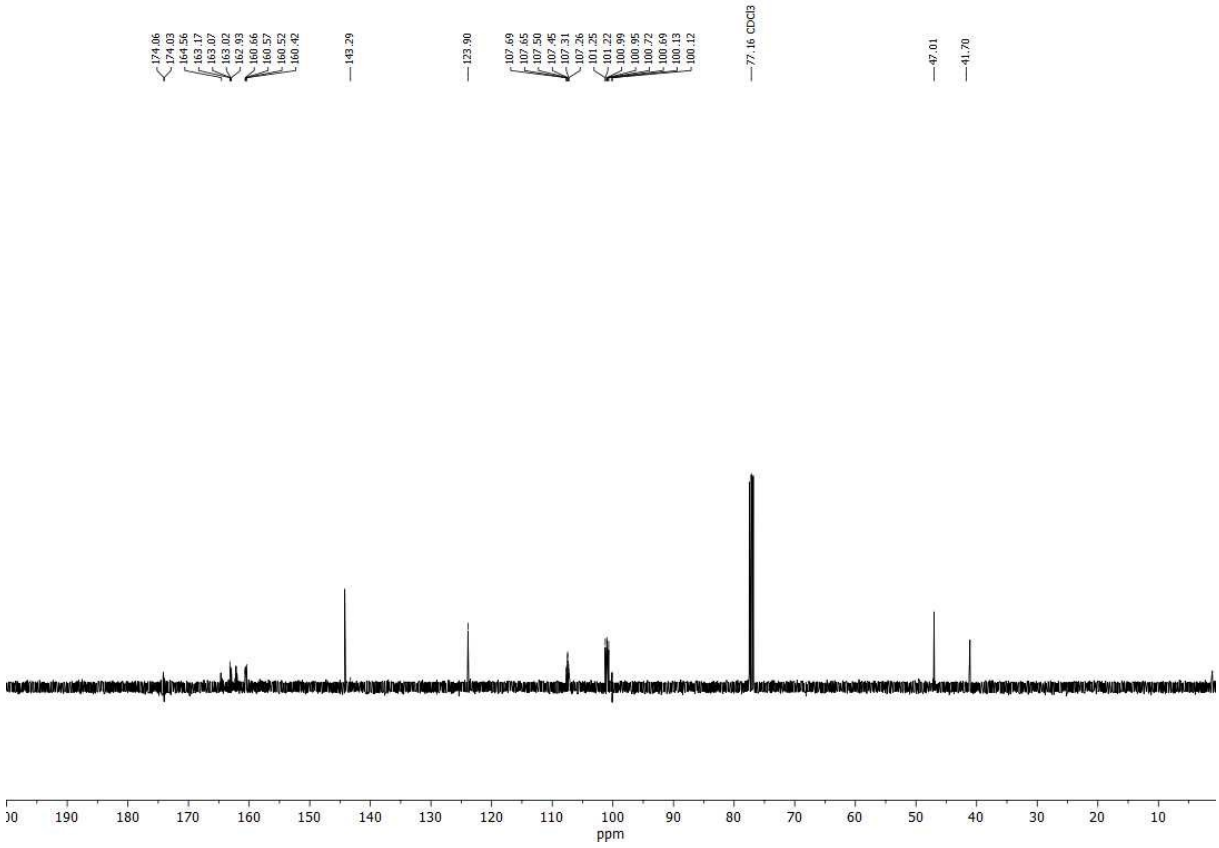

Figure S27: ^{13}C NMR of TF_3TA in $CDCl_3$.

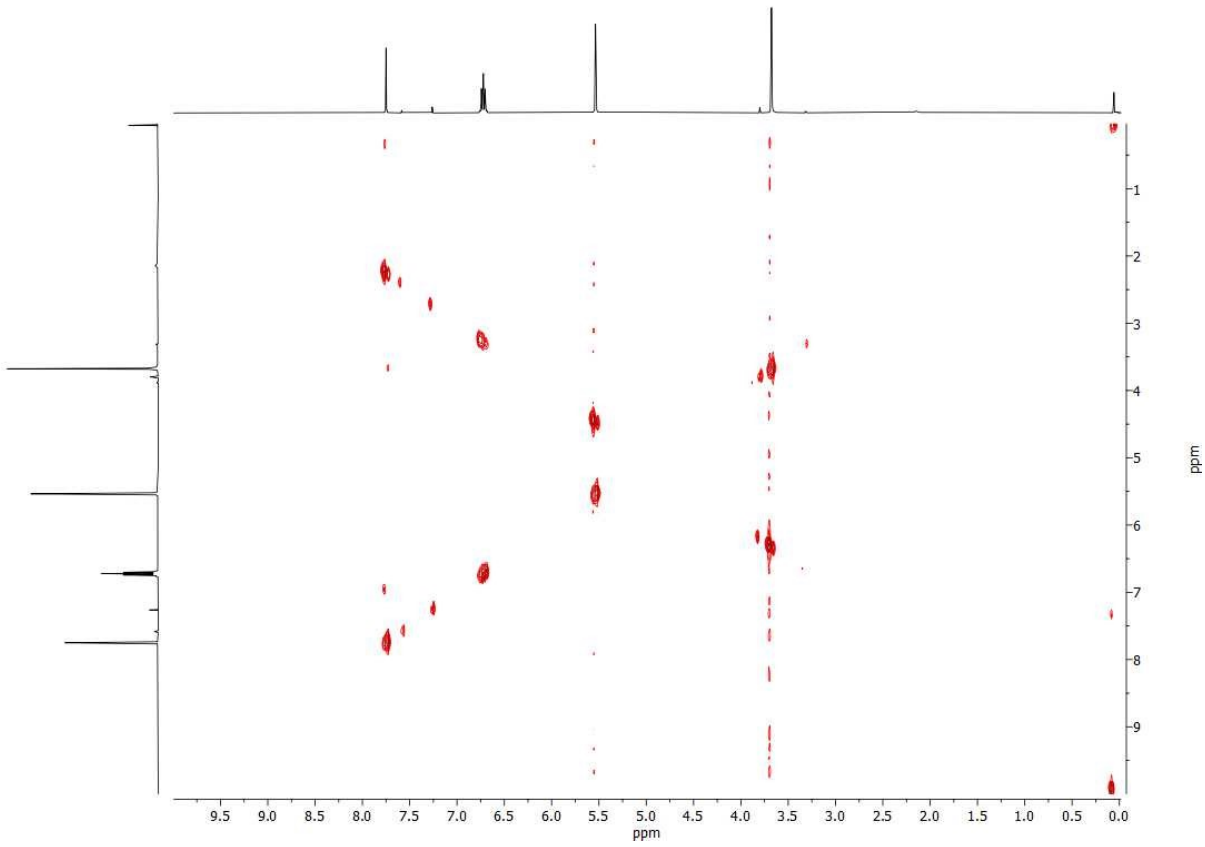

Figure S28: ^{1}H ^{1}H COSY NMR of TF_3TA in $CDCl_3$.

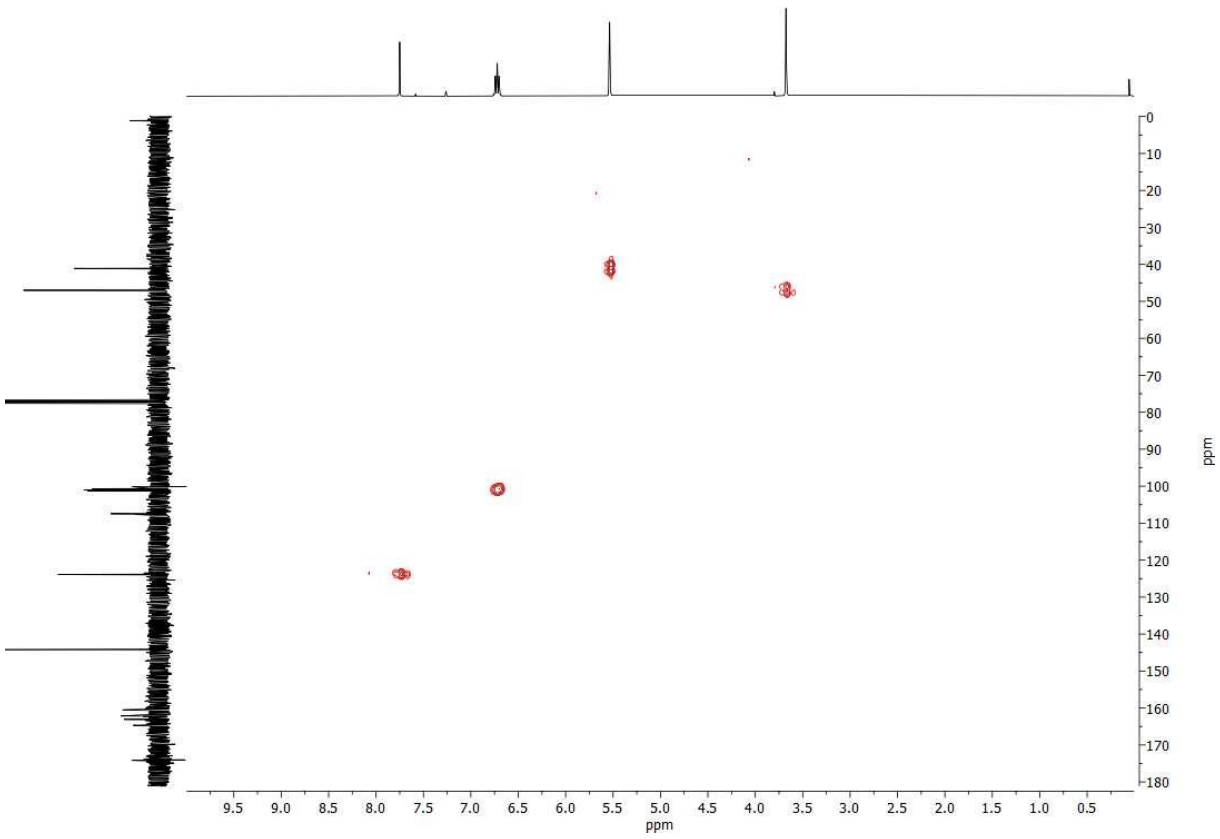

Figure S29: ^{1}H ^{13}C HMQC NMR of TF_3TA in $CDCl_3$.

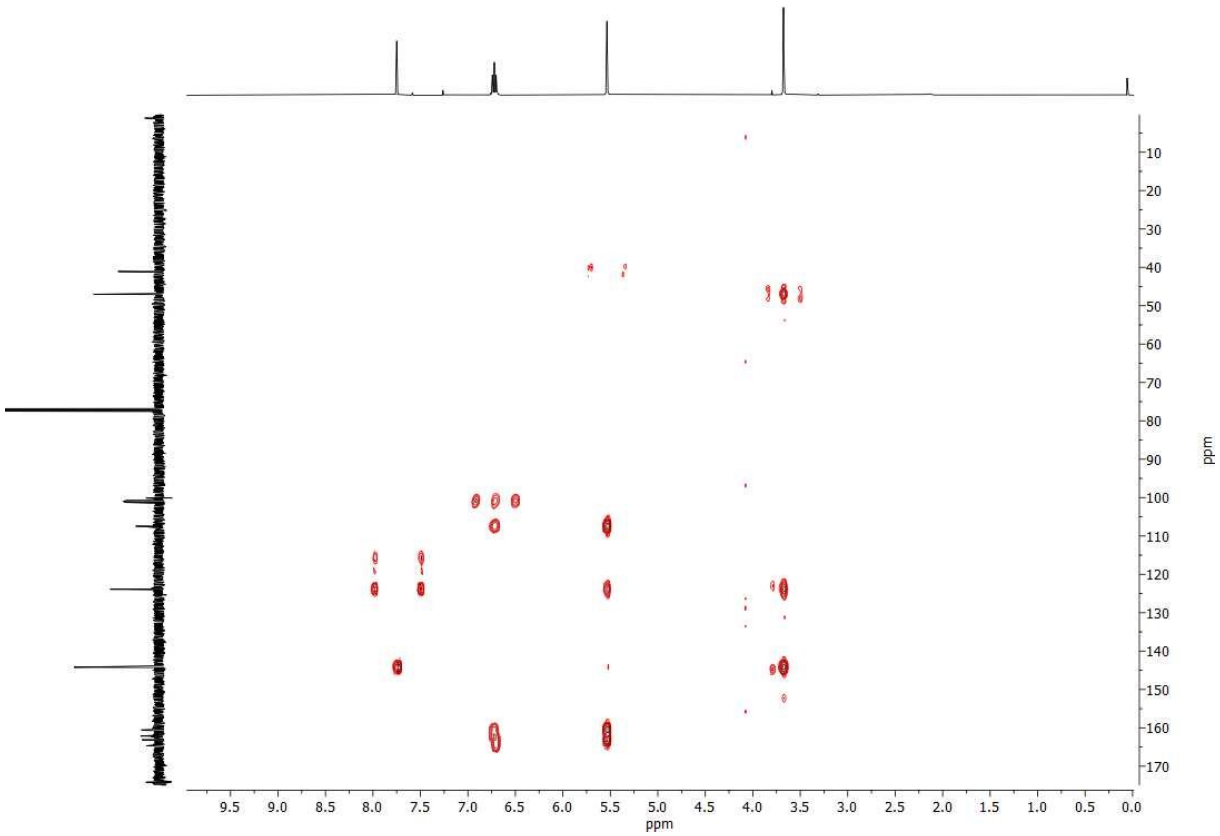

Figure S30: ^{1}H ^{13}C HMBC NMR of TF_3TA in $CDCl_3$

References

[1] D. Schweinfurth, J. Klein, S. Hohloch, S. Dechert, S. Demeshko, F. Meyer, B. Sarkar, *Dalton Trans.* **2013**, *42*, 6944-6952.

[2] F. Weisser, S. Plebst, S. Hohloch, M. van der Meer, S. Manck, F. Führer, V. Radtke, D. Leichnitz, B. Sarkar, *Inorg. Chem.* **2015**, *54*, 4621-4635.

[3] D. Schweinfurth, S. Demeshko, S. Hohloch, M. Steinmetz, J. G. Brandenburg, S. Dechert, F. Meyer, S. Grimme, B. Sarkar, *Inorg. Chem.* **2014**, *53*, 8203-8212.

[4] G. R. Fulmer, A. J. M. Miller, N. H. Sherden, H. E. Gottlieb, A. Nudelman, B. M. Stoltz, J. E. Bercaw, K. I. Goldberg, *Organometallics* **2010**, *29*, 2176-2179.

[5] G. M. Sheldrick, *SHELXS-97, Program for Crystal Structure Solution and Refinement,* **1997**, University of Göttingen, Germany.

[6] G. Sheldrick, *Acta Crystallogr., Sect. A* **2008**, *64*, 112-122.

[7] G. M. Sheldrick, *SADABS Ver. 2008/1, SADABS. Program for Empirical Absorption Correction* **2012**, University of Göttingen, Germany.

[8] G. M. Sheldrick, *SHELXL Version 2014/7, Program for Chrystal Structure Solution and Refinement* **2014**, University of Göttingen, Germany.

[9] G. Sheldrick, *Acta Crystallogr. Sect. C* **2015**, *71*, 3-8.

[10] A. Spek, *J. Appl. Crystallogr.* **2003**, *36*, 7-13.

[11] SAINT+, *Data Integration Engine, Version 8.27b*©, Bruker AXS, Madison, Wisconsin, USA, 1997-2012.

[12] G. A. Bain, J. F. Berry, *J. Chem. Educ.* **2008**, *85*, 532.

[13] P. Neugebauer, D. Bloos, R. Marx, P. Lutz, M. Kern, D. Aguilà, J. Vaverka, O. Laguta, C. Dietrich, R. Clérac, J. van Slageren, *Phys. Chem. Chem. Phys.* **2018**, *20*, 15528-15534.

[14] J. Pietruszka, G. Solduga, *Eur. J. Org. Chem.* **2009**, *2009*, 5998-6008.

[15] R. Ahlrichs, M. Bär, M. Häser, H. Horn, C. Kölmel, *Chem. Phys. Lett.* **1989**, *162*, 165-169.

[16] O. Treutler, R. Ahlrichs, *J. Chem. Phys.* **1995**, *102*, 346-354.

[17] M. Von Arnim, R. Ahlrichs, *J. Comput. Chem.* **1998**, *19*, 1746-1757.

[18] R. A. Kendall, T. H. D. Jr., R. J. Harrison, *J. Chem. Phys.* **1992**, *96*, 6796-6806.

[19] F. Weigend, A. Köhn, C. Hättig, *J. Chem. Phys.* **2002**, *116*, 3175-3183.

[20] C. Hättig, G. Schmitz, J. Koßmann, *Phys. Chem. Chem. Phys.* **2012**, *14*, 6549-6555.

[21] K. A. Peterson, T. B. Adler, H.-J. Werner, *J. Chem. Phys.* **2008**, *128*, 084102.

[22] C. Hättig, *Phys. Chem. Chem. Phys.* **2005**, *7*, 59-66.

[23] K. E. Yousaf, K. A. Peterson, *J. Chem. Phys.* **2008**, *129*, 184108.

[24] F. Neese, *WIREs Comput. Mol. Sci.* **2012**, *2*, 73-78.

[25] M. Ernzerhof, G. E. Scuseria, *J. Chem. Phys.* **1999**, *110*, 5029-5036.

[26] F. Weigend, R. Ahlrichs, *Phys. Chem. Chem. Phys.* **2005**, *7*, 3297-3305.

[27] E. Caldeweyher, S. Ehlert, A. Hansen, H. Neugebauer, S. Spicher, C. Bannwarth, S. Grimme, *J. Chem. Phys.* **2019**, *150*, 154122.